

This discussion paper is/has been under review for the journal Atmospheric Chemistry and Physics (ACP). Please refer to the corresponding final paper in ACP if available.

# The isotopic composition of methane in the stratosphere: high-altitude balloon sample measurements

T. Röckmann<sup>1,2</sup>, M. Brass<sup>1,2</sup>, R. Borchers<sup>3</sup>, and A. Engel<sup>4</sup>

<sup>1</sup>Institute for Marine and Atmospheric Research Utrecht, Utrecht University, Utrecht, The Netherlands

<sup>2</sup>Atmospheric Physics Division, Max Planck Institute for Nuclear Physics, Heidelberg, Germany

<sup>3</sup>Planets and Comets Department, Max Planck Institute for Solar System Research, Katlenburg-Lindau, Germany

<sup>4</sup>Institute for Atmospheric and Environmental Sciences, J. W. Goethe University, Frankfurt, Germany

Received: 17 February 2011 – Accepted: 31 March 2011 – Published: 19 April 2011

Correspondence to: T. Röckmann (t.roeckmann@uu.nl)

Published by Copernicus Publications on behalf of the European Geosciences Union.

## The isotopic composition of methane in the stratosphere

T. Röckmann et al.

Title Page

Abstract

Introduction

Conclusions

References

Tables

Figures

⏪

⏩

◀

▶

Back

Close

Full Screen / Esc

Printer-friendly Version

Interactive Discussion

## Abstract

The isotopic composition of stratospheric methane has been determined on a large suite of air samples from stratospheric balloon flights covering subtropical to polar latitudes and a time period of 16 yr. 154 samples were analyzed for  $\delta^{13}\text{C}$  and 119 samples for  $\delta\text{D}$ , increasing the previously published dataset for balloon borne samples by an order of magnitude, and more than doubling the total available stratospheric data (including aircraft samples) published to date. The samples also cover a large range in mixing ratio from tropospheric values near 1800 ppb down to only 250 ppb, and the strong isotope fractionation processes accordingly increase the isotopic composition up to  $\delta^{13}\text{C} = -14\text{‰}$  and  $\delta\text{D} = +190\text{‰}$ , the largest enrichments observed for atmospheric  $\text{CH}_4$  so far. When analyzing and comparing kinetic isotope effects (KIEs) derived from single balloon profiles, it is necessary to take into account the residence time in the stratosphere in combination with the observed mixing ratio and isotope trends in the troposphere, and the range of isotope values covered by the individual profile. Temporal isotope trends can also be determined in the stratosphere and compare reasonably well with the tropospheric trends. The effects of chemical and dynamical processes on the isotopic composition of  $\text{CH}_4$  in the stratosphere are discussed in detail. Different ways to interpret the data in terms of the relative fractions of the three important sink mechanisms (reaction with OH,  $\text{O}(^1\text{D})$  and Cl, respectively), and their limitations, are investigated. The classical approach of using global mean KIE values can be strongly biased when profiles with different minimum mixing ratios are compared. Approaches for more local KIE investigations are suggested. It is shown that any approach for a formal sink partitioning from the measured data severely underestimates the fraction removed by OH, which is likely due to the insensitivity of the measurements to the kinetic fractionation in the lower stratosphere. Attempts can be made to correct for the lower stratospheric sink bias, but full quantitative interpretation of the  $\text{CH}_4$  isotope data in terms of the three sink reactions requires a global model.

### The isotopic composition of methane in the stratosphere

T. Röckmann et al.

Title Page

Abstract

Introduction

Conclusions

References

Tables

Figures



Back

Close

Full Screen / Esc

Printer-friendly Version

Interactive Discussion



## 1 Introduction

In the well-mixed troposphere, the CH<sub>4</sub> mixing ratio and its isotopic composition are determined by the principal balance between the sources (and their isotopic signatures) and sinks (and the corresponding kinetic fractionation factors) (Stevens and Rust, 1982; Quay et al., 1999; Miller et al., 2002). For a long-lived gas as methane, this leads to rather stable mixing ratio and isotope values throughout the troposphere that are modulated by the seasonal variations in the production and destruction rates and long-term temporal trends, resulting from disequilibrium of production and removal (Stevens and Rust, 1982; Lowe et al., 1997; Bergamaschi et al., 1998, 2000, 2001; Quay et al., 1999; Tyler et al., 1999; Miller et al., 2002; Tarasova et al., 2006).

In the stratosphere the situation is different, since the only source for stratospheric methane is the tropospheric flux into the stratosphere, occurring mainly in the tropics. In the absence of in situ sources CH<sub>4</sub> mixing ratio decrease strongly due to the removal in the stratosphere by the three chemical (1st order) reactions with OH, O(<sup>1</sup>D) and Cl (Wahlen et al., 1989; Wahlen, 1993; Brenninkmeijer et al., 1995; Irion et al., 1996; Sugawara et al., 1997; Ridal and Siskind, 2002; McCarthy et al., 2003; Rice et al., 2003). Consequently, the CH<sub>4</sub> mixing ratio and its isotopic composition in an air parcel is dependent on the reaction with these three radicals (chemical removal) on the one hand and its pathway through the stratosphere (physical transport, dynamics) on the other hand. In general, the longer the residence time of an air mass in the stratosphere, the more it is processed photochemically and the more CH<sub>4</sub> has been removed.

As CH<sub>4</sub> is not fully oxidized in the stratosphere, but a significant fraction returns to the troposphere, the isotope effects in the stratosphere have a significant effect on the tropospheric CH<sub>4</sub> isotope budget (Gupta et al., 1996; McCarthy et al., 2001; Wang et al., 2002).

Only a limited number of data on isotopic composition of stratospheric methane have been previously published. Sugawara et al. (1997) presented one δ<sup>13</sup>C profile from a balloon flight over Japan in 1994 and Rice et al. (2003) presented δ<sup>13</sup>C and δD values

### The isotopic composition of methane in the stratosphere

T. Röckmann et al.

Title Page

Abstract

Introduction

Conclusions

References

Tables

Figures

⏪

⏩

◀

▶

Back

Close

Full Screen / Esc

Printer-friendly Version

Interactive Discussion

from various ER-2 flights (high-altitude aircraft) between 1996–2000 up to 21 km. Furthermore, Brenninkmeijer et al. (1995, 1996) published few  $\delta^{13}\text{C}$  data obtained on aircraft flights between New Zealand and Antarctica.

In this paper we present data from 13 stratospheric balloon flights, which increase the number of balloon observations in the literature by more than an order of magnitude and the number of total published data for the stratosphere by a factor of more than 2.

## 2 Short review of stratospheric dynamics and its effect on tracer distributions

After air enters the stratosphere, mainly in the tropical region, it is transported upwards and polewards and descends at higher latitudes. The turnaround time for this global meridional circulation, the so-called Brewer-Dobson-circulation (BDC, Dobson et al., 1946; Brewer, 1949) is several years for the middle and upper stratosphere. The major force for driving the BDC is breaking of planetary-scale Rossby-waves in the middle and the upper stratosphere, which leads to a net poleward and downward transport at mid and high latitudes (McIntyre and Palmer, 1983; Andrews et al., 1987; Holton et al., 1995). At lower altitudes, exchange between the TTL and the extratropical lowermost stratosphere is achieved through quasi-horizontal transport associated with synoptic-scale eddies. The lower stratospheric transport from tropics to mid-latitudes is realized within about 3–4 months (Boering et al., 1996).

The combination of this net residual circulation and isentropic mixing determines the global distribution of long-lived tracers in the stratosphere. The surfaces of constant mixing ratio (isopleths) are a result of these two effects. First, the meridional net circulation lifts the tracer isopleth in the tropics and depresses them at high-latitudes and second, the quasi-horizontal mixing equilibrates the tracer distribution along the isentropes. For long-lived tracers, the fast quasi-horizontal mixing forms rapid exchange surfaces, common to all (sufficiently) long-lived tracers, on which local deviations are homogenized globally. As a consequence two long-lived tracers will form a compact relation in a tracer:tracer plot, i.e., ideally a single curve for the correlation of their

### The isotopic composition of methane in the stratosphere

T. Röckmann et al.

Title Page

Abstract

Introduction

Conclusions

References

Tables

Figures

⏪

⏩

◀

▶

Back

Close

Full Screen / Esc

Printer-friendly Version

Interactive Discussion



## The isotopic composition of methane in the stratosphere

T. Röckmann et al.

Title Page

Abstract

Introduction

Conclusions

References

Tables

Figures



Back

Close

Full Screen / Esc

Printer-friendly Version

Interactive Discussion

5 mixing ratios (Holton, 1986; Mahlman et al., 1986; Plumb and Ko, 1992). This idealized model is sometimes referred to as “global mixing scheme”. It has successively been extended to better describe the situation in the tropics (tropical pipe with subtropical barriers, splitting the common global isopleth into two hemispheric “surf zones” and a tropical part, Plumb, 1996; Andrews et al., 2001) and include mid-latitude backflows (reentrainment) into the tropics (“leaky” tropical pipe, which allows recirculation of air, Avallone and Prather, 1996; Volk et al., 1996; Neu and Plumb, 1999).

10 The polar vortices are seasonal thermodynamic structures, which are not included in these general global transport schemes. The radiative cooling in the polar night and the stronger downward forcing from the BDC in winter leads to a large-scale subsidence of air from the upper stratosphere and even mesosphere, which stays substantially isolated from extra-vortex air. Thus, the vortex edge, similar to the subtropical barrier, is characterised by strong horizontal tracer and potential vorticity gradients and the tracer isopleths are no more “almost parallel” to isentropes, indicating that the fast quasi-horizontal isentropic mixing is disturbed. Several mechanisms are known or discussed for interaction between vortex and extra-vortex air. Waugh et al. (1997) showed the occurrence of “anomalous mixing” lines, i.e., deviating from the general compact tracer:tracer relation, and related them to end-member mixing between vortex and mid-latitudes. Plumb et al. (2000) offered two alternative mechanisms, a “continuous weak mixing” through the vortex edge and the intrusion of extra-vortex air in a single (or multiple) event(s) throughout the phase of descent, and its subsequent vertical redistribution inside the vortex. Such an intrusion was used in Engel et al. (2006) to explain the enclosure of mesospheric air in stratospheric balloon samples. With increasing solar heating after the polar night, the latitudinal temperature gradient, circumpolar jet, wave activities, and vortex isolation decrease and vortex air dissipates into the surrounding extra-vortex region (WMO, 2003). How the dynamical properties of the stratosphere affect the mixing ratio and isotopic composition of CH<sub>4</sub> will be discussed in detail in Sects. 5 and 6.3.

### 3 Experimental

High-altitude samples (up to 35 km) from stratospheric balloon borne air samplers were provided by the Max-Planck-Institut (MPI) für Sonnensystemforschung (formerly Max-Planck-Institut für Aeronomie), Katlenburg-Lindau, Germany and the Institut für Atmosphäre und Umwelt (formerly Institut für Meteorologie und Geophysik, Universität Frankfurt, Germany). The samplers from both groups consist of 15 electro-polished stainless steel tubes immersed into liquid neon at a temperature of 27 K, but differ especially in the intake design (Schmidt et al., 1987). The sampling tubes have an internal volume of about  $0.5 \text{ dm}^3$  that is filled to pressures between  $\sim 5$  to 50 bar (at room temperature). The vertical sampling resolution is usually about 1 km, sampling latitudes are essentially invariant, and longitude variations can be a few degrees, depending on the prevailing zonal winds during sample collection.

The MPI group had stored a large number of stratospheric air samples from scientific balloon flights covering more than a decade (1987–1999) as stratospheric air archive. Those samples were made available for isotope analysis on long-lived greenhouse gases. From 2000 to 2003, samples from 5 more stratospheric flights with the BON-BON cryogenic sampler operated by the Universität Frankfurt group were analyzed. Those samples were measured within few months after the flight. Table 2 gives an overview of the exact sampling dates and locations.

Mixing ratio and isotopic composition of the air samples were determined on a high-precision continuous flow isotope ratio mass spectrometry system (Brass and Röckmann, 2010). The samples are analyzed automatically relative to a laboratory standard air cylinder that is usually measured after each two samples. Most samples were attached to the analytical system directly from the original sampling containers, only a subset of samples was first expanded into 2 L volume stainless steel flasks and analyzed later. For  $\delta^{13}\text{C}$  analysis we use the peak integration routine of the standard ISODAT software package, for  $\delta\text{D}$  an improved peak integration software has been developed (Brass and Röckmann, 2010).

## The isotopic composition of methane in the stratosphere

T. Röckmann et al.

Title Page

Abstract

Introduction

Conclusions

References

Tables

Figures

⏪

⏩

◀

▶

Back

Close

Full Screen / Esc

Printer-friendly Version

Interactive Discussion



## 4 Results

### 4.1 General classification of flight profiles

Figure 1a shows the full set of methane mixing ratio profiles obtained from the balloon flights. As outlined in the introduction, mixing ratios decrease from tropospheric levels with altitude and latitude in the stratosphere. This is due to CH<sub>4</sub> destruction related to the photochemical processing of stratospheric air as it rises upward and poleward in the Brewer-Dobson circulation. The extent of chemical removal is clearly different for the individual profiles and the samples split into three groups, roughly according to the flight latitude, i.e., high latitudes (polar, here Arctic), mid latitudes and subtropics.

Generally, the  $\delta^{13}\text{C}$  and  $\delta\text{D}$  vertical profiles mirror the mixing ratio profiles (higher mixing ratio corresponds to lower  $\delta$ -values) and therefore they generally show similar structural variations (Fig. 1b and c). The  $\delta$ -values increase with altitude and latitude. Vortex air, with its very low CH<sub>4</sub> content, shows the highest enrichments. The degree of this enrichment depends on the relative strengths of the involved chemical sink processes.

While previous measurements (Rice et al., 2003) cover mixing ratios between 700–1800 ppb with  $\delta^{13}\text{C}$  reaching from tropospheric values  $\sim -48\text{‰}$  to  $-34\text{‰}$ , and  $\delta\text{D}$  from  $-90\text{‰}$  to  $\sim +26\text{‰}$ , respectively, this work considerably extends the range of available data, to CH<sub>4</sub> mixing ratios down to  $\sim 250$  ppb, corresponding to values up to  $-13.7\text{‰}$  for  $\delta^{13}\text{C}$  and  $+190\text{‰}$  for  $\delta\text{D}$ .

#### 4.1.1 Polar profiles

The Arctic samples (all collected using Kiruna as operational base) show additional differences for different sampling seasons. The winter samples (KIR-92-01, -02, -03, KIR-00-01, KIR-03-03) reflect the presence of the polar vortex. Air that descends in the vortex has undergone massive oxidation. These profiles are characterised by the occurrence of very low methane mixing ratios (down to  $\sim 250$  ppb) and strong isotope

### The isotopic composition of methane in the stratosphere

T. Röckmann et al.

Title Page

Abstract

Introduction

Conclusions

References

Tables

Figures

⏪

⏩

◀

▶

Back

Close

Full Screen / Esc

Printer-friendly Version

Interactive Discussion



enrichments. The spring and summer profiles (KIR-95-03, KIR-03-06) are similar to mid-latitudinal profiles.

The balloon profile KIR-03-03 shows a distinct feature, i.e., at the higher altitudes the CH<sub>4</sub> mixing ratio increases and  $\delta^{13}\text{C}$  and  $\delta\text{D}$  decrease again with height. A detailed analysis of this flight, using several tracers, shows that at least the fourth and fifth sample from the top show clear mesospheric characteristics like high CO and H<sub>2</sub> mixing ratios (compare Engel et al., 2006). Above those “mesospheric” samples, the air exhibits stratospheric characteristics again, and the methane mixing ratio and isotope data suggest that mid-latitudinal air is mixed into the resolving vortex from above.

#### 4.1.2 Mid-Latitude profiles

Four profiles from mid-latitudes are available (ASA-93-09, GAP-99-06, ASA-01-10, and ASA-02-09). Three flights took place in autumn and to some degree can be regarded as a stratospheric background. Stratosphere-troposphere-exchange is minimal in autumn, photochemistry is decreased compared to summer and dynamical activity starts to intensify with the change from the summer to the winter circulation. All four profiles show wave structures in the vertical distribution of mixing ratio and isotopic composition with altitude, which indicate large-scale dynamical effects that disturb the smooth vertical evolution. In general, the mixing ratio and isotope values of the mid latitude flights are in the range of the Arctic summer profile (KIR-03-06), esp. for altitudes above 20 km.

#### 4.1.3 Subtropical profiles

The subtropical region is represented by samples from two balloon flights from Hyderabad, India, HYD-87-03 and HYD-99-04. Methane mixing ratios are rather constant up to the tropopause at 18 km and slightly decrease above the tropopause, followed by a significant decrease starting at 20–23 km. Only 5 samples were still available from the HYD-87-03 flight, resulting in two groups of similar characteristics. Thus, this dataset

### The isotopic composition of methane in the stratosphere

T. Röckmann et al.

Title Page

Abstract

Introduction

Conclusions

References

Tables

Figures

⏪

⏩

◀

▶

Back

Close

Full Screen / Esc

Printer-friendly Version

Interactive Discussion



alone holds only limited information. Compared to HYD-99-04 the HYD-87-043 profile is shifted to lower mixing ratios and looks similar to a mid-latitudinal profile. One has to take into account that 12 yr passed between the two profiles. An age correction that takes the tropospheric trend into account will be applied later.

5 Sample HYD-99-04/15 is the highest altitude subtropical sample with a mixing ratio  $\sim 1200$  ppb and an extremely high  $\delta^{13}\text{C}$ -value (for a sample with 1200 ppb). When the balloon samples are compared to  $\text{CH}_4:\text{N}_2\text{O}$  tracer correlations for different latitude bins taken from (Michelsen et al., 1998), the tracer:tracer-plot identifies HYD-99-04/15 as  
10 the only deep tropical sample in the balloon set. However, this was one of the samples that were only available as an aliquot (not the original balloon sample container) and were analysed for  $\delta^{13}\text{C}$  only at the very beginning of measurement. Also the original container had rather low pressure. Since experimental problems cannot be excluded, this sample will not be interpreted further.

## 4.2 Isotope – mixing ratio correlations

15 It is obvious from Fig. 1 that there is considerable variability between the individual flight profiles. However, the variations in mixing ratio and isotopic composition are closely correlated, and it is useful and common to investigate isotope results as isotope – mixing ratio correlations (Fig. 2). Two points are remarkable in these correlations. First, each flight profile shows up as a single line and second, isotope-mixing ratio  
20 correlations are relatively stable over the full period of time, in different seasons and at various latitudinal regions (subtropics, mid-latitudes and polar). Thus, most of the variation observed in the vertical profiles disappears when  $\delta$ -values are discussed on the mixing ratio scale (as alternative height coordinate) and the correlation curves can be regarded as a (quasi) steady state functions for  $\delta^{13}\text{C}(c)$  and  $\delta\text{D}(c)$ . Here and in the  
25 following,  $c$  represents the mixing ratio.

The first observation reflects the previous finding that compact stratospheric tracer-tracer correlations occur for trace gases whose chemical removal time constants are larger than the transport time constants (Plumb and Ko, 1992), which is the case for

### The isotopic composition of methane in the stratosphere

T. Röckmann et al.

Title Page

Abstract

Introduction

Conclusions

References

Tables

Figures



Back

Close

Full Screen / Esc

Printer-friendly Version

Interactive Discussion



the individual CH<sub>4</sub> isotopologues. Thus this property can be explained by the global mixing scheme. The second observation shows the global validity of this scheme and that it is not strongly variable in time. This is expected, since CH<sub>4</sub> is a long-lived trace gas with only small temporal trends. Consequently, no major changes in dynamics in the stratosphere and/or changes in the chemical sinks are observed.

Nevertheless, two areas of variability can be easily identified in Fig. 2: first, there is increased variability in both  $\delta$ -values for methane mixing ratios  $< \sim 1000$  ppb, which is mainly vortex or vortex edge air. For this region the assumptions of Plumb and Ko (1992) fail, since at the vortex edge mixing ratio the quasi-horizontal mixing on an isentrope is not fast enough to equilibrate mixing ratio variations. In the inner vortex region the time scale for vertical advection is of the same size as horizontal transport across the edge. Furthermore, the vortex undergoes dramatic changes over the seasons (it forms, breaks up and resolves).

Secondly, there is comparably large scatter for  $\delta D$  at high methane mixing ratios, i.e. near the tropopause, where the  $\delta D(c)$  correlations are slightly shifted between individual flights. This point will be further investigated below.

#### 4.2.1 Isotope – isotope correlations

Figure 3 shows the isotope – isotope correlation between  $\delta D$  and  $\delta^{13}C$ . In such a plot, air that is a result of mixing between two air parcels is found on a straight line connecting these two parcels. Such a linear mixing correlation in fact fits the mid-latitude data points well. In contrast, the vortex samples) significantly deviate from this straight (mid-latitudinal) correlation. For a global fit, the data was binned in 0.5%  $\delta^{13}C$  intervals to reduce the statistical weight of the more abundant higher mixing ratio (lower  $\delta$ -values) samples. When the point with highest isotope enrichment (sample KIR-03-03/12) is disregarded, a parabolic fit of the form

$$\delta D = -0.0557 \cdot (\delta^{13}C)^2 + 3.9017 \cdot \delta^{13}C + 229.39, r^2 = 0.9978 \quad (1)$$

### The isotopic composition of methane in the stratosphere

T. Röckmann et al.

Title Page

Abstract

Introduction

Conclusions

References

Tables

Figures



Back

Close

Full Screen / Esc

Printer-friendly Version

Interactive Discussion



## The isotopic composition of methane in the stratosphere

T. Röckmann et al.

Title Page

Abstract

Introduction

Conclusions

References

Tables

Figures

⏪

⏩

◀

▶

Back

Close

Full Screen / Esc

Printer-friendly Version

Interactive Discussion



fits the data well without systematic structure in the residuals (Fig. 3c). The most interesting feature of the fit in Fig. 3b is its monotonically decreasing slope. This implies a decrease of D fractionation compared to  $^{13}\text{C}$  fractionation at higher total enrichments (see below). Pure Rayleigh fractionation processes would actually show a slightly increasing slope, which is due to the non-linearity of the Rayleigh fractionation equation, so other process must contribute. Given the large differences in the fractionation constants associated with the three chemical sink reactions (see below), the overall monotonous decrease can only be caused by a continuously decreasing strength of the OH sink and the related increase of the  $\text{O}(^1\text{D})$  and Cl strength (and to a minor degree shifting from Cl to  $\text{O}(^1\text{D})$ ).

The two vortex samples that fall below and above the mesospheric enclosure in flight KIR-03-03 deviate from this general description. According to (Engel et al., 2006), sample KIR-03-03/8, has typical characteristics of upper stratospheric air from the mid-latitudes and indeed it accurately falls onto the mid-latitudinal mixing line and marks its most enriched end-point (Fig. 3a). The second sample, KIR-03-03/12, is much more difficult to interpret, as it is completely isolated from the other samples in the isotope:isotope plane. It will be further discussed below.

### 4.3 Comparison to previous datasets

#### 4.3.1 $\delta^{13}\text{C}$ comparison

In the published literature, there is a clear difference between the  $\delta^{13}\text{C}$  data from Sugawara et al. (1997) (balloon) and Rice et al. (2003) (ER-2 flights), which has been attributed either to the different location/time period of sampling or to lab-specific calibration procedures (Rice et al., 2001). When compared to our data, the Rice et al. (2003) data (1996–2000) fall in the range of the Arctic aircraft and balloon samples from 2003. At the same time, the KIR-92-01 profile agrees well with the Sugawara et al. (1997) data from the 1994 balloon profile. Thus, the new comprehensive measurements indicate that the difference between the Sugawara et al. (1997) and Rice et al. (2003) data is likely not an analytical artefact and probably due to the temporal trends.

### 4.3.2 $\delta D$ comparison

In comparison to Rice et al. (2003) the  $\delta D$  values presented here are about 10‰ heavier. The difference appears to decrease towards lower mixing ratios and may disappear at 700 ppb. Several processes may contribute to the discrepancy. A fractionation in the sampling procedure is unlikely for our analyses, as samples from different sampling devices agree well. Given the fact that both  $\delta D$  datasets cover large regions of the stratosphere, it is unlikely that the observed difference indicates a real atmospheric difference. Most likely the deviation originates from different, lab-specific calibration scales. This typically leads to systematic deviations. Ideally, these deviations are constant, but they can also increase or decrease with mixing ratio, as observed. Because of this non-constant deviation, the ER-2 data discussed by Rice et al. (2003) and McCarthy et al. (2003) show a more pronounced relative vertical increase of  $\delta D$  in the stratosphere, i.e., a generally higher slope of  $\delta D(c)$  relation, and consequently slightly higher KIE<sup>D</sup>-values are reported by Rice et al. (2003) and McCarthy et al. (2003).

## 5 Chemical and physical effects on the isotopic composition

### 5.1 Chemical isotope fractionation in the removal reactions

In the stratosphere methane is oxidised by OH, O(<sup>1</sup>D) and Cl. Due to slightly different reaction rate constants for the different isotopologues, chemical removal by these reactions leads to a shift in the isotope ratio of the residual material, which can be described by the Rayleigh fractionation equation.

$$\ln\left(\frac{\delta+1}{\delta_0+1}\right) = \left(\frac{1}{\text{KIE}} - 1\right) \ln\left(\frac{c}{c_0}\right) \quad (2)$$

$\delta$  and  $\delta_0$  are the initial and final  $\delta$ -values and  $c_0$  and  $c$  are the initial and final mixing ratios. KIE is the kinetic isotope effect, defined as the ratio of the reaction rate constants

## The isotopic composition of methane in the stratosphere

T. Röckmann et al.

Title Page

Abstract

Introduction

Conclusions

References

Tables

Figures

⏪

⏩

◀

▶

Back

Close

Full Screen / Esc

Printer-friendly Version

Interactive Discussion



for the light ( $k$ ) and heavy ( $k'$ ) isotopologue

$$\text{KIE} = \frac{k}{k'} = \frac{k(\text{light isotopologue})}{k(\text{heavy isotopologue})} \quad (3)$$

A normal kinetic isotope effect is characterised by  $k > k'$ . In case of a constant KIE, it can be determined from the slope of a Rayleigh fractionation plot (Eq. 2). The corresponding fractionation constant  $\varepsilon$  is defined as

$$\varepsilon = \text{KIE} - 1 \quad (4)$$

As for  $\delta$ -values, the numerical values of  $\varepsilon$  are usually stated in per mille. Note that in many publications  $\varepsilon$  is defined as  $\alpha - 1$  (where  $\alpha = k'/k = (\text{KIE})^{-1}$ ). The same symbol  $\varepsilon$  is used in both cases, which are not equivalent.

Saueressig et al. (2001) determined the KIE values and their temperature dependence for the reactions of OH, O(<sup>1</sup>D) and Cl with the three major isotopologues <sup>12</sup>CH<sub>4</sub>, <sup>13</sup>CH<sub>4</sub>, <sup>12</sup>CH<sub>3</sub>D (Table 1). In Rice et al. (2003) a modified Rayleigh framework is derived for the more complicated situation of three simultaneous sink reactions, taking into account the three major methane isotopologues, <sup>12</sup>CH<sub>4</sub>, <sup>13</sup>CH<sub>4</sub> and <sup>12</sup>CH<sub>3</sub>D. In this case, the combined isotope effect can be written as the sum of the individual isotope effects weighted by the fraction  $a_Y$  of methane oxidised by Y (Y = OH, O(<sup>1</sup>D), Cl).

$$\text{KIE}_{\text{eff}}^X = a_{\text{OH}}\text{KIE}_{\text{OH}}^X + a_{\text{O}^1\text{D}}\text{KIE}_{\text{O}^1\text{D}}^X + a_{\text{Cl}}\text{KIE}_{\text{Cl}}^X, X = {}^{13}\text{C}, \text{D} \quad (5)$$

with  $a_{\text{OH}} + a_{\text{O}^1\text{D}} + a_{\text{Cl}} = 1$ . If the KIEs for each loss reaction are known (Table 1) and the effective KIEs have been determined, in this framework it is possible to formally derive the relative sink fractions ( $a_{\text{OH}}$ ,  $a_{\text{O}^1\text{D}}$  and  $a_{\text{Cl}}$ ) from the measurement of both  $\text{KIE}_{\text{eff}}$  values, where  $\text{KIE}_{\text{eff}}$  is the effective KIE measured in the stratosphere.

$$\begin{aligned} \text{KIE}_{\text{eff}}^{13\text{C}} &= a_{\text{OH}}\text{KIE}_{\text{OH}}^{13\text{C}} + a_{\text{O}^1\text{D}}\text{KIE}_{\text{O}^1\text{D}}^{13\text{C}} + a_{\text{Cl}}\text{KIE}_{\text{Cl}}^{13\text{C}} \\ \text{KIE}_{\text{eff}}^{\text{D}} &= a_{\text{OH}}\text{KIE}_{\text{OH}}^{\text{D}} + a_{\text{O}^1\text{D}}\text{KIE}_{\text{O}^1\text{D}}^{\text{D}} + a_{\text{Cl}}\text{KIE}_{\text{Cl}}^{\text{D}} \\ 1 &= a_{\text{OH}} + a_{\text{O}^1\text{D}} + a_{\text{Cl}} \end{aligned} \quad (6)$$

## The isotopic composition of methane in the stratosphere

T. Röckmann et al.

Title Page

Abstract

Introduction

Conclusions

References

Tables

Figures

⏪

⏩

◀

▶

Back

Close

Full Screen / Esc

Printer-friendly Version

Interactive Discussion



Equation (6) is a set of 3 linear equations for 3 unknowns and can also be formulated as vector equation

$$\begin{pmatrix} \text{KIE}_{\text{eff}}^{13\text{C}} \\ \text{KIE}_{\text{eff}}^{\text{D}} \\ 1 \end{pmatrix} = \begin{pmatrix} \text{KIE}_{\text{OH}}^{13\text{C}} & \text{KIE}_{\text{O}^{1\text{D}}}^{13\text{C}} & \text{KIE}_{\text{Cl}}^{13\text{C}} \\ \text{KIE}_{\text{OH}}^{\text{D}} & \text{KIE}_{\text{O}^{1\text{D}}}^{\text{D}} & \text{KIE}_{\text{Cl}}^{\text{D}} \\ 1 & 1 & 1 \end{pmatrix} \begin{pmatrix} a_{\text{OH}} \\ a_{\text{O}^{1\text{D}}} \\ a_{\text{Cl}} \end{pmatrix} \quad (7)$$

In the real atmosphere the situation is more complicated. The distribution of the radicals and therefore the fractions vary with altitude, latitude, time and season and it is not straightforward to deduce a representative  $\text{KIE}_{\text{eff}}$  from the measured  $\delta$ -values and mixing ratios (see below). Furthermore, dynamical effects have to be taken into account, which affect the isotope signals. Nevertheless, due to mixing, the observed KIE-values in the stratosphere are fairly constant, which allows to determine empirically a “global mean”  $\text{KIE}_{\text{mean}}$  from the slope of a linear fit to a Rayleigh plot of a discrete number of samples.

$$\frac{1}{\text{KIE}_{\text{mean}}} - 1 = \text{linearfitslope} \left( \frac{y_j = \ln [(\delta_j + 1) / (\delta_{\text{initial}} + 1)]}{x_j = \ln [(c_j) / (c_{\text{initial}})]} \right) \quad (8)$$

Still this “mean” approach has several deficiencies, which so far have not been discussed in detail in the literature. The limitations of using mean KIEs to determine a mean sink partitioning will be further investigated in Sect. 7.

## 5.2 Transport and mixing processes

### 5.2.1 Diffusive mixing

In addition to chemistry, also mixing has a strong effect on the isotopic composition of the long-lived trace gases in the stratosphere. Eddy-diffusion is a major reason why  $\text{KIE}_{\text{eff}}$  is not directly accessible from stratospheric measurements. The observed *apparent* KIE,  $\text{KIE}_{\text{app}}$ , is always smaller than the *effective* KIE in the actual removal

## The isotopic composition of methane in the stratosphere

T. Röckmann et al.

Title Page

Abstract

Introduction

Conclusions

References

Tables

Figures

⏪

⏩

◀

▶

Back

Close

Full Screen / Esc

Printer-friendly Version

Interactive Discussion



reactions (see e.g. Rahn et al., 1998; Kaiser et al., 2002). The lower value of  $KIE_{app}$  reflects the continuous dilution by diffusive mixing processes. In the following two dynamical parameters  $f^{13C}$  and  $f^D$  quantify the influence of transport and/or mixing on KIE.

$$f^{13C} := \frac{KIE_{app}^{13C} - 1}{KIE_{eff}^{13C} - 1} = \frac{\varepsilon_{app}^{13C}}{\varepsilon_{eff}^{13C}}; \quad f^D := \frac{KIE_{app}^D - 1}{KIE_{eff}^D - 1} = \frac{\varepsilon_{app}^D}{\varepsilon_{eff}^D} \quad (9)$$

Thus,  $f = 1$  characterises an undisturbed Rayleigh fractionation process, whereas mixing and diffusion generally lead to lower values of  $f$ , i.e.  $KIE_{app} < KIE_{eff}$ .  $f^{13C}$  and  $f^D$  can be included in the equation to derive the sink partitioning as follows:

$$\begin{pmatrix} a_{OH} \\ a_{O^1D} \\ a_{Cl} \end{pmatrix} = \begin{pmatrix} KIE_{OH}^{13C} & KIE_{O^1D}^{13C} & KIE_{Cl}^{13C} \\ KIE_{OH}^D & KIE_{O^1D}^D & KIE_{Cl}^D \\ 1 & 1 & 1 \end{pmatrix}^{-1} \begin{pmatrix} 1 + \frac{KIE_{eff}^{13C} - 1}{f^{13C}} \\ 1 + \frac{KIE_{eff}^D - 1}{f^D} \\ 1 \end{pmatrix} \quad (10)$$

A consequence of the steady-state in the global mixing scheme is that the net vertical trace gas fluxes are purely diffusive (Plumb, 1996). For this specific case a simplified discussion on the resulting isotope profile was already presented in Kaye (1987) (see also Erikson, 1965). In this idealised 1-D-diffusive steady-state model  $f$ -values between 0.5 and 1 are theoretically possible (independent of molecule and/or isotope), where  $f = 0.5$  characterises the so-called diffusion-limited case, which describes the situation expected for the stratosphere (Rahn et al., 1998; Kaiser et al., 2002). Thus, only half of the expected effective KIE is apparently observed. It will be shown below that in general this 1-D-diffusive model already predicts the stratospheric fractionation surprisingly well.

**The isotopic composition of methane in the stratosphere**

T. Röckmann et al.

Title Page

Abstract

Introduction

Conclusions

References

Tables

Figures



Back

Close

Full Screen / Esc

Printer-friendly Version

Interactive Discussion



## 5.2.2 Two-end-member mixing

A second type of mixing of relevance to the stratosphere is two-end-member mixing, where two reservoirs (or parts of them) with distinct characteristics are homogenized. This type of mixing represents the prototype of irreversible mixing processes. It is known that for normal KIEs, which result in isotope-mixing ratio correlations as shown in Fig. 2, mixing of two different points on a single Rayleigh fractionation curve (the end-members) will always produce a mixture with isotope characteristics that fall below the Rayleigh fractionation curve (Kaiser et al., 2002). Therefore the observed  $KIE_{app}$  will always be lower than  $KIE_{eff}$  (i.e.  $f < 1$ ) in the presence of atmospheric mixing processes, as shown in the following: we choose two end members with mixing and isotope ratios  $c_1, r_1$  and  $c_2, r_2$ , respectively, that are derived from an initial parcel  $c_0, r_0$  via a pure Rayleigh fractionation process with  $\varepsilon_{Rayleigh}$ . Relative to the initial mixing ratio  $c_0$ , the resulting mix then has a fractionation constant of

$$\varepsilon_{mix}(x) = \frac{\ln(C_1 \cdot (1 - x \cdot C_2))}{\ln(R_1 \cdot (1 - x \cdot R_2))} - 1 \quad (11)$$

with constants

$$C_1 = \frac{c_1}{c_0}; R_1 = \left(\frac{c_1}{c_0}\right)^{m+1} \quad (12)$$
$$C_2 = 1 - \frac{c_2}{c_1}; R_2 = 1 - \left(\frac{c_2}{c_1}\right)^{m+1}$$

$0 \leq x \leq 1$  denotes the fraction of  $c_2$  and determines the resulting mixing ratio  $c_{mix}$  through

$$c_{mix} = c_1 \cdot (1 - x) + c_2 \cdot x \quad (13)$$

Figure 4 shows an example for the effect of two-end-member mixing, expressed in terms of  $f$ -values. This means that  $\varepsilon$  of the mixture is compared to the initial  $\varepsilon_{Rayleigh}$ , i.e.  $f = \varepsilon_{mix} / \varepsilon_{Rayleigh}$ . The resulting “ $f$ -valley” is the deeper and broader the more different the two end-members are, and a very large difference has been chosen for

12054

### The isotopic composition of methane in the stratosphere

T. Röckmann et al.

Title Page

Abstract

Introduction

Conclusions

References

Tables

Figures

⏪

⏩

◀

▶

Back

Close

Full Screen / Esc

Printer-friendly Version

Interactive Discussion



illustration. The  $f$ -values are slightly different for the individual isotopes. To emphasize this difference we define  $f_r$  as the ratio of  $f^D$  and  $f^{13C}$ .

$$f_r := \frac{f^D}{f^{13C}} \quad (14)$$

Figure 4 also shows that  $f_r$  is not constant for two-end-member mixing.

Large-scale mixing or stirring processes greatly increase the contact surfaces between different air masses and therefore will favour irreversible mixing. Typically samples from an area where mixing occurs can be well described by two end-member-mixing, where physical quantities and/or trace gas/isotope content are derived from a weighted mix of the two involved reservoirs. An example is the period of polar vortex breakup, where vortex air is mixed into mid-latitude air.

### 5.2.3 Example: mixing across the vortex edge

For a more realistic example of end-member mixing, we calculate mixing across the polar vortex edge. The isotopic evolution of a representative tropospheric air parcel with  $c_0 = 1780$  ppb,  $\delta^{13C}_0 = -47.5\text{‰}$  and  $\delta D_0 = -81\text{‰}$  is calculated using  $KIE^{13C} = 1.0155$  and  $KIE^D = 1.150$  (based on  $\varepsilon^{13C} = 31\text{‰}$ ,  $\varepsilon^D = 300\text{‰}$  and  $f = 0.5$ ). The mixing ratio (and thus isotope) profiles differ for two profiles that represent vortex and mid-latitude air. Starting from 12 km altitude with 1780 ppb the mixing ratio decrease linearly to 630 ppb in the mid-latitudes and to 280 ppb in the vortex at 30 km. Air from these two profiles is then mixed on equal heights assuming with relative vortex fractions of 0.2, 0.4, 0.5, 0.6 and 0.8 for all altitudes. This results in profiles of the mixtures, from which mean KIE values can be derived and compared to the effective KIEs in terms of  $f$  values.

The KIE values of the mixed profiles are not constant and  $KIE_{\text{mean}}$  is derived from a subset of altitudes and characterised by the lowest mixing ratio (mix) included. E.g., in Fig. 5 the data points at the highest mixing ratio are derived from only the two lowermost profile points.

## The isotopic composition of methane in the stratosphere

T. Röckmann et al.

Title Page

Abstract

Introduction

Conclusions

References

Tables

Figures

⏪

⏩

◀

▶

Back

Close

Full Screen / Esc

Printer-friendly Version

Interactive Discussion



The effects for  $^{13}\text{C}$  and D are almost equal ( $1 \times 10^{-8} < |f_r - 1| < 5 \times 10^{-4}$ ) and  $f$  is necessarily smaller than 0.5 (Fig. 5). As expected,  $f$  decreases towards higher altitudes (lower mixing ratios), where the two reservoirs differ more.

This example clearly shows that, via mixing, dynamical processes can have a distinct influence on the isotope distribution and the  $f$ - and  $\delta$ -values get sensitive to atmospheric dynamics. Importantly, such mixing will always lead to  $f < 0.5$ , when the  $\text{KIE}_{\text{app}}$  values of the mixing air masses themselves are at the diffusion-limited extreme ( $f = 0.5$ ) individually. Mixing across the vortex edge is likely an extreme example, as the air masses are rather different, but it is certainly relevant for the atmosphere.

## 6 Mean fractionation factor

According to Eq. (8), a mean KIE for the respective profile can be determined from a linear fit in a double-logarithmic plot such as Fig. 7. The results of those mean KIE values are shown in Table 3. The corresponding fractionation factors vary for the individual flights over the range 12–17‰ for  $\varepsilon^{13}\text{C}$  and 122–160‰ for  $\varepsilon^{\text{D}}$ .

In general the fits are of very good quality and give high accuracy KIE values with the following exceptions. The HYD-87-03 profile basically consists of only two groups of points. For HYD-99-04 half of the profile shows nearly constant (tropospheric) values, which effectively reduces the number of useful samples. Additionally, both HYD profiles occupy only a small  $c$ -interval in the  $\delta(c)$  relations. Also for  $\text{KIE}^{\text{D}}$  (ASA-02-09) the regression coefficient is lower, likely due to the limited number of samples analysed for  $\delta\text{D}$ .

Previously published mean KIE values are listed in Table 4 for comparison. The  $\text{KIE}^{13}\text{C}$  derived by Sugawara et al. (1997), the only previously published result from a stratospheric balloon flight, is similar to the subtropical (HYD-99-04) result from this study. The overall average of Rice et al. (2003) is in very good agreement with the mid-latitudinal average of this work. Including the results of highly depleted polar air leads to slightly lower values for  $\varepsilon^{\text{D}}$ .

## The isotopic composition of methane in the stratosphere

T. Röckmann et al.

Title Page

Abstract

Introduction

Conclusions

References

Tables

Figures



Back

Close

Full Screen / Esc

Printer-friendly Version

Interactive Discussion



The samples reported in Brenninkmeijer et al. (1995, 1996) were collected in the southern hemispheric lower stratosphere (10–12 km) at mid and high latitudes. They cover only a small range in mixing ratio (1620–1690 ppb). No comparable data set is available from this work. Nevertheless, similar KIEs are observed, if the new dataset is restricted to high mixing ratio samples only.

A long-term temporal trend in the KIE-values is not discernible from the data in Table 3. Nevertheless, one further factor needs to be corrected for, namely the correction of the bias introduced by the presence of the tropospheric temporal trends.

## 6.1 Tropospheric trend correction by mean age

The “instantaneous” evaluation of mean KIEs as discussed so far relates the highest altitude sample, which has resided in the stratosphere for years, to an initial value that is taken from the lowermost sample, which only recently entered the stratosphere or is still located in the upper troposphere. This method will only reflect the true chemical and dynamical stratospheric fractionation in the absence of tropospheric trends. If, in contrast, tropospheric trends exist, then the higher altitude stratospheric samples are related to initial tropospheric values that do not reflect the conditions at the time the sample entered the stratosphere. The deviation is the bigger the larger the tropospheric trends are and the longer the sample of interest already resided in the stratosphere, i.e., the longer the time it took to reach the point of sampling after entering the stratosphere. Kida (1983) introduced the concept of stratospheric “mean age”. This concept describes a stratospheric air mass as a collection of individual isolated air parcels. Each parcel has been transported on its own path associated with a characteristic transport time and thus the air mass has a spectrum of transport times, of which the mean value defines the mean (stratospheric) age. While the age distribution is quite sharp for lower stratospheric tropical air, it gets wider with increasing altitudes due to mixing (for further details see (Hall and Plumb, 1994; Waugh and Rong, 2002) and references therein).

## The isotopic composition of methane in the stratosphere

T. Röckmann et al.

Title Page

Abstract

Introduction

Conclusions

References

Tables

Figures

⏪

⏩

◀

▶

Back

Close

Full Screen / Esc

Printer-friendly Version

Interactive Discussion



When the stratospheric mean age is known and the atmospheric trend can be approximated by a linear function, each sample (SMP) can be related to a corrected upper tropospheric value by

$$\ln\left(\frac{\delta(\text{SMP}) + 1}{\delta_T(t_s - \Gamma(\text{SMP})) + 1}\right) = \left(\frac{1}{\text{KIE}} - 1\right) \ln\left(\frac{c(\text{SMP})}{c_T(t_s - \Gamma(\text{SMP}))}\right) \quad (15)$$

where  $\Gamma$  is the mean age of the sample,  $t_s$  the date of sampling and  $\delta_T(t)$  and  $c_T(t)$  the tropospheric time series of the  $\delta$  value and mixing ratio.

$\text{N}_2\text{O}$  is a well-suited age indicator for several reasons. It has only surface sources and a very small (negligible) seasonal variation. Moreover, it is inert in the troposphere and long-lived in the stratosphere. The tropospheric mixing ratio  $c(\text{N}_2\text{O})_T$  increases linearly in time, thus it is well-defined and well-known. The stratospheric mean age for most samples presented here was already derived from the  $\text{N}_2\text{O}$  measurements by (Kaiser et al., 2006), yielding the formula:

$$\Gamma_{\text{N}_2\text{O}}\left(\frac{c(\text{N}_2\text{O})}{c(\text{N}_2\text{O})_T}\right) = -(7.43 \pm 0.34) \left(\frac{c(\text{N}_2\text{O})}{c(\text{N}_2\text{O})_T}\right)^3 + (3.68 \pm 0.56) \left(\frac{c(\text{N}_2\text{O})}{c(\text{N}_2\text{O})_T}\right)^2 - (1.94 \pm 0.28) \left(\frac{c(\text{N}_2\text{O})}{c(\text{N}_2\text{O})_T}\right) + (5.69 \pm 0.04) \quad (16)$$

The tropospheric trend for the  $\text{N}_2\text{O}$  mixing ratio  $c(\text{N}_2\text{O})_T$  is taken from the mean annual trend observed at Mace Head (AGAGE), Ireland, from April 1994 to September 2003, derived from monthly averaged  $\text{N}_2\text{O}$  mixing ratio measurements.

$$c(\text{N}_2\text{O})_T(t_s) = 0.765 \text{ ppbyr}^{-1} \cdot (t_s - 1994) + 311.21 \text{ ppb} \quad (17)$$

Based on the  $\text{N}_2\text{O}$  derived mean age ( $\Gamma_{\text{N}_2\text{O}}$ ), a relation between  $\text{CH}_4$  mixing ratio and  $\Gamma_{\text{N}_2\text{O}}$  (Fig. 8) is derived and then used to interpolate  $\Gamma$  from the  $\text{CH}_4$  mixing ratio, when  $\text{N}_2\text{O}$  data are missing. To stay consistent for all samples in Fig. 8 only  $\Gamma(c(\text{CH}_4)) = \Gamma_{\text{CH}_4}$  is used in the following. The differences between  $\Gamma_{\text{CH}_4}$  and  $\Gamma_{\text{N}_2\text{O}}$  do not cause significant changes in the determination of KIE. Neglecting the small methane trend, the mean age is thus given as:

$$\Gamma_{\text{CH}_4}(c(\text{CH}_4)[\text{ppm}]) = -2.131c^3 + 2.460c^2 - 1.1c + 5.788r^2 = 0.9975 \quad (18)$$

12058

**The isotopic composition of methane in the stratosphere**

T. Röckmann et al.

Title Page

Abstract

Introduction

Conclusions

References

Tables

Figures

⏪

⏩

◀

▶

Back

Close

Full Screen / Esc

Printer-friendly Version

Interactive Discussion



Some slightly negative values for  $\Gamma_{\text{CH}_4}$  relate to samples with mixing ratios slightly higher than the assumed tropospheric background values. Those samples are either from the troposphere or samples strongly influenced by tropospheric air and/or seasonal variation in  $\text{CH}_4$  mixing ratio. The negative ages  $\Gamma_{\text{CH}_4}$  do not lead to major changes in mean KIE.

The tropospheric  $\text{CH}_4$  trend  $c_{\text{T}}(t)$  used in (15) is constructed from measurements at Mace Head, Ireland,  $40^\circ \text{N}$  between May 1994 and September 2003 (Simpson et al., 2002), extrapolated back to 1984 with growth rates from (Dlugokencky et al., 1998), yielding

$$c(\text{CH}_4)[\text{ppb}] = k_0 + k_1 \cdot \text{yr} + k_2 \cdot \text{yr}^2 \quad \text{with} \quad k_0 = -1766.707, k_1 = 1766.723, k_2 = -0.441245 \quad (19)$$

Isotope trends are derived from the upper tropospheric data from the balloon samples themselves and fixed to the tropospheric sample HYD-99-04/3 ( $c = 1766$  ppb,  $\delta^{13}\text{C} = -47.30\text{‰}$  and  $\delta\text{D} = -81.3\text{‰}$ ) on reference date  $t_{\text{ref}} = 1999.445$  (26 April 1999).

$$\delta^{13}\text{C}_{\text{T}}(t) = -47.30 + 0.034/\text{yr} \cdot (t - t_{\text{ref}})[\text{VPDB}] \quad (20)$$

$$\delta\text{D}_{\text{T}}(t) = -81.3 + 0.86/\text{yr} \cdot (t - t_{\text{ref}})[\text{VSMOW}]$$

The mean age corrected fractionation constants  $\varepsilon^{13}\text{C}$  and  $\varepsilon^{\text{D}}$  derived by linear fits of Eq. (15) using the trends Eqs. (20) and (19) are listed in Table 5 together with the absolute and relative change from the uncorrected values (Table 3).

In total the corrected KIEs are quite insensitive to parameter changes. Of course, the magnitudes of tropospheric  $\delta$ -trends are of relevance. Further the correction is sensitive to the shape of the function that describes the mean age relation  $\Gamma_{\text{CH}_4}$ , whereas shifting  $\Gamma$  by  $\pm 1$  yr or stretching it for 1 additional year does not significantly change the results.

In general the mean age correction leads to higher KIE-values, and the effect increases towards lower latitudes. In tendency, it amplifies the  $\text{KIE}^{\text{D}}$  signal relative to  $\text{KIE}^{13\text{C}}$ . This is related to the relative size of the tropospheric  $\delta$ -trend, which for  $\delta^{13}\text{C}$

## The isotopic composition of methane in the stratosphere

T. Röckmann et al.

[Title Page](#)[Abstract](#)[Introduction](#)[Conclusions](#)[References](#)[Tables](#)[Figures](#)[⏪](#)[⏩](#)[◀](#)[▶](#)[Back](#)[Close](#)[Full Screen / Esc](#)[Printer-friendly Version](#)[Interactive Discussion](#)

## The isotopic composition of methane in the stratosphere

T. Röckmann et al.

Title Page

Abstract

Introduction

Conclusions

References

Tables

Figures

⏪

⏩

◀

▶

Back

Close

Full Screen / Esc

Printer-friendly Version

Interactive Discussion

is small. The effects of the age correction are largest at the subtropical locations for two reasons. Looking at the evolution of  $\Gamma_{\text{CH}_4}$  in Fig. 8, it is clear that changes will be largest for mixing ratios between 1700 ppb and 1200 ppb, where the mean age strongly increases with decreasing mixing ratios. Here, the initial value used in the Rayleigh fractionation formula is most strongly altered, whereas at the low mixing ratio range (<800 ppb), where the mean age does not vary much, the initial value is rather constant for the whole interval.

Figure 9 shows the uncorrected (a) and the mean age corrected (b) mean KIE values in direct comparison. After applying the correction the mean KIEs are grouped more closely together in the KIE - KIE plane. Still, the remaining scatter of about 3‰ for KIE<sup>13C</sup> and ~30‰ for KIE<sup>D</sup> is surprisingly high for an assumed mean global stratospheric quantity probed at several locations. Part of this scatter is caused by the latitudinal cut-off bias (see next section), i.e., the limitation of the subtropical data to the high mixing ratio range. However, variations associated with seasonal vortex dynamics (e.g. stirring and mixing after vortex breakdown, KIR-92 flight series) are of similar size, but of course spatially more confined (only within the group of vortex flights). In the remainder of this paper only the mean age corrected fractionation constants are discussed.

### 6.2 Latitudinal mixing ratio cut-off bias and non-constant apparent KIE

As the apparent fractionation is not constant over the entire range of mixing ratios, the value of the minimum mixing ratio  $c_{\text{min}}$  of each sample profile strongly affects the mean KIEs. This is shown in Fig. 10, where the mean KIE is plotted as function  $c_{\text{min}}$  for all flights. Due to the strong latitudinal mixing ratio gradient in the stratosphere,  $c_{\text{min}}$  at altitudes of about 30 km (typical maximum altitude of the balloon flights) differs for the different regions. It is around 1200 ppb for the subtropics, 650 ppb–900 ppb for mid latitudes and polar regions without vortex influence, and ~300 ppb for vortex flights. Since KIE increases with decreasing mixing ratio, this leads to a bias when

comparing profiles with different  $c_{\min}$ . We call this effect latitudinal cut-off bias. The higher minimum mixing ratio is the major reason why the subtropical KIE  $^{13}\text{C}$  values in Table 3 and Table 5 are significantly lower than at mid latitudes and in the Arctic region.

Due to this latitudinal cut-off bias only the mean fractionation factors from profiles with similar minimal mixing ratio  $c_{\min}$  should be compared directly. It should be noted, however, that typically the sample density of vortex flights is rather low in the c-interval covered by subtropical flights, i.e. down to 1200 ppb. Figure 11 shows an evaluation of the individual profiles where successively the highest points are truncated (“bottom-up” profiles). It is clear that the mean fractionation factor  $\varepsilon_{\text{mean}}$  for each individual profile depends on  $c_{\min}$ . Figure 11 shows that when the latitudinal cut-off bias is removed, the differences between the latitudinal regions are very small. This means that dynamical effects supersede chemical sink effects and lead to smooth variations of both, methane mixing ratio and isotopic composition.

### 6.3 Global interpretation from the chemical and dynamical perspective

Figure 6 shows theoretical Rayleigh fractionation curves for a reasonably realistic, atmospherically weighted, fractionation constant  $\varepsilon_{\text{eff}}^{13}\text{C} = 31\text{‰}$ , and  $\varepsilon_{\text{app}}^{13}\text{C} \sim \varepsilon_{\text{eff}}^{13}\text{C} / 2 = 15.5\text{‰}$  estimated for the diffusion limited case ( $f = 0.5$ ). The good agreement of the Rayleigh fractionation calculations using  $\varepsilon_{\text{app}}^{13}\text{C} = 15.5\text{‰}$  suggest that the observed isotope:mixing ratio correlations result from a balance between fractionation due to chemical loss and mixing processes, primarily eddy-diffusion. Nevertheless, some simplifications are of importance for the further discussion. First, the assumption of purely diffusive vertical fluxes: already the tropical pipe model (Plumb, 1996) predicts advective components in these fluxes. Thus, the purely diffusive model is less suitable for the subtropics and the vortices than for the mid-latitudes. It can be expected that periods with stronger wave activity, leading to a stronger BDC and therefore stronger advection are less well represented than periods with weaker wave activity. In that sense the mid-latitudinal stratosphere in autumn (lowest wave activity in the NH) is most suitable and may be

## The isotopic composition of methane in the stratosphere

T. Röckmann et al.

Title Page

Abstract

Introduction

Conclusions

References

Tables

Figures

⏪

⏩

◀

▶

Back

Close

Full Screen / Esc

Printer-friendly Version

Interactive Discussion



called “stratospheric background”. Second, single, height independent loss rates are assumed, which corresponds to a constant  $KIE_{\text{eff}}$ . However, this is not true for  $\text{CH}_4$  with its three different sink reactions, particularly concerning the lower stratosphere where the OH-sink is clearly dominant. Third, the assumption of steady-state conditions is not always valid. In particular the occurrence of the polar vortex and its dynamical life-cycle is neither part of the global mixing scheme nor of the tropical pipe model.

Advective mixing and the influence of the polar vortex are likely responsible for the remaining variability around the quasi-constant isotope-mixing ratio correlation curve. The corresponding deviations are spatially and/or temporally confined and therefore result in a scatter. Points falling below the average curve represent air parcels that have experienced more than average mixing. The opposite is true for points above the curve. In general, the interpretation of the  $\text{CH}_4$  isotope signals is in agreement with the situation as discussed for  $\text{N}_2\text{O}$  (Kaiser et al., 2006).

## 7 Limitations of global mean sink partitioning

In this section it will be investigated whether/how the derived mean KIE can be related to the mean relative strength of the three stratospheric sink reactions. It is already clear from Eq. (10) that the results will depend on the concrete choice of values for  $f^{13\text{C}}$  and  $f^{\text{D}}$ .

### 7.1 Sink partitioning – results from previous models

Two extended 2-D-model studies on the isotopic composition of stratospheric methane have been published. Bergamaschi et al. (1996), updated in Saueressig et al. (2001) used a photochemical 2-D-model to predict the distribution of OH, O(<sup>1</sup>D) and Cl in the stratosphere. The model is able to reproduce the  $\delta^{13\text{C}}(c)$  fractionation profile from Sugawara et al. (1997). According to this model, in the middle and upper stratosphere ( $p < 10$  hPa) Cl accounts for ~20% of the  $\text{CH}_4$  sink strength at low and mid-latitudes

## The isotopic composition of methane in the stratosphere

T. Röckmann et al.

Title Page

Abstract

Introduction

Conclusions

References

Tables

Figures

⏪

⏩

◀

▶

Back

Close

Full Screen / Esc

Printer-friendly Version

Interactive Discussion



and for ~30% at high latitudes.  $O(^1D)$  is estimated to cause 30% of the loss in the tropics and mid-latitudes (Fig. 5 in Bergamaschi et al., 1996). The relative global mean sink strengths and the corresponding effective KIEs for these model results are for the year 1993 (C. Brühl, MPI für Chemie, Germany, personal communication, 2003):

$$(a_{OH}^G, a_{O^1D}^G, a_{Cl}^G) = (0.41, 0.33, 0.26)$$

$$5 \quad KIE_{eff}^{13C} = 25.39 \quad (21)$$

$$KIE_{eff}^D = 328.6$$

The second modelling study from McCarthy et al. (2003) yields similar numbers for the sink partitioning.

In an inverse approach, the model results from Eq. (21) can be used in Eq. (10) to calculate  $f^{13C}$  and  $f^D$  from the average KIE measurements (Table 5). To take the cut-off bias in the determination of mean KIEs into account, this was done separately for the different groups of flights.

It is obvious from Table 6 that  $f^{13C}$  and  $f^D$  differ significantly. Whereas all  $f^{13C}$  exceed 0.5,  $f^D$  is always below 0.5, and consequently and  $f_r < 1$ . Whereas values of  $f^D < 0.5$  cannot be excluded per se, they are not expected because the diffusion limited case of 1-D diffusive theory,  $f = 0.5$  (Kaiser et al., 2002), fits the data so well. The general finding  $f_r < 1$  shows that compared to what is expected from  $^{13}C$  and previous models, the observed signal in deuterium is strongly attenuated. We will refer to this fact as  $KIE^D$ -discrimination. The  $KIE^D$ -discrimination increases towards higher latitudes, which is mainly caused by the latitudinal cut-off bias in the determination of the mean KIE. Additionally, the attenuation increases when deuterium depleted vortex air (compare the vortex branch of the  $\delta D : \delta^{13}C$  relation) is included in the sample set.

The observed  $KIE^D$ -discrimination and the fact that  $f^D < 0.5$  point towards general inconsistencies between the radical abundances as predicted in atmospheric models

**The isotopic composition of methane in the stratosphere**

T. Röckmann et al.

Title Page

Abstract

Introduction

Conclusions

References

Tables

Figures

⏪

⏩

◀

▶

Back

Close

Full Screen / Esc

Printer-friendly Version

Interactive Discussion



Discussion Paper | Discussion Paper | Discussion Paper | Discussion Paper | Discussion Paper

and the approach of deriving sink partitioning from mean KIEs via Eq. (10). In particular, the OH sink fraction of 41% as predicted by the models cannot be reconciled with the derived mean KIEs under the condition  $f_r \sim 1$ , i.e., the observed D enrichment is too low compared to the  $^{13}\text{C}$  enrichment.

## 7.2 Conceptual limitations of the partitioning approach and the origin of the KIE<sup>D</sup>-discrimination

The approach of deducing the sink partitioning from Eq. (10) is strictly applicable only for an idealized removal process where all three sink processes occur simultaneously in a well-mixed volume, i.e., KIE is constant. However, the stratospheric sink processes do not occur simultaneously. The OH sink clearly dominates in the lower stratosphere and the other two sinks gain in importance with altitude. This partly sequential removal of  $\text{CH}_4$  is generally masked by the fact that diffusive mixing removes most of the resulting gradients in the apparent fractionation constants. This on the one hand precludes deriving details of the altitude distribution of the different sink processes in the stratosphere from isotope data, but also limits the use of the mean fractionation constants in Eq. (10). This can be demonstrated in a simple calculation: the isotope fractionation of a typical tropospheric air sample ( $c = 1750$  ppb,  $\delta^{13}\text{C} = -47.5\text{‰}$ ,  $\delta\text{D} = -81\text{‰}$ ) is calculated when three times 300 ppb are subsequently removed by all three chemical sinks, but in different order. Table 7 lists the final  $\delta$  values for all permutations of the sinks and clearly the final enrichments are very different. Although the perfect sequential removal in this idealized experiment exaggerates the issue, it illustrates that the order of removal is important for the final isotopic composition. In this idealized experiment we then use the final isotope composition to calculate again the apparent KIEs and the relative sink fractions (under the condition  $f = 1$ ) for each scenario. Theoretically the sink partitioning should be calculated to (1/3; 1/3; 1/3), but this result is only retrieved for case 7 when the removal in fact occurs simultaneously.

The results in Table 7 show that the mean KIE, and thus the sink partitioning derived using the mean KIE approach, is pathway dependent. A fairly realistic sink partitioning

## The isotopic composition of methane in the stratosphere

T. Röckmann et al.

Title Page

Abstract

Introduction

Conclusions

References

Tables

Figures



Back

Close

Full Screen / Esc

Printer-friendly Version

Interactive Discussion





$x^{\text{US}}$  is the fractional loss in the middle/upper stratosphere and  $1 - x^{\text{US}}$  the fractional loss in the lower stratosphere.  $a^{\text{US}}$  is the sink partitioning derived from Eq. (10) and  $a^{\text{LS}}$  the unknown partitioning of the lower stratosphere.

We assume that for the middle/upper stratospheric sink Eq. (10) is applicable and

$$f_r = 1, \text{ i.e., } f^{13\text{C}} = f^{\text{D}} = f.$$

The middle stratospheric sink partitioning can then be written as

$$a_j = a_{j1} \cdot \left(1 + \frac{1}{f} \left(\text{KIE}_{\text{app}}^{13\text{C}} - 1\right)\right) + a_{j2} \cdot \left(1 + \frac{1}{f} \left(\text{KIE}_{\text{app}}^{\text{D}} - 1\right)\right) + a_{j3} \quad (23)$$

where  $a_{j(1,2,3)}$  are the constant coefficients of the inverse KIE matrix in Eq. (10).

Equation (23) can be simplified by defining constants  $A_j$  and  $K_j$ , where  $K_j$  is a function of the measured apparent fractionation

$$a_j = \sum_{i=1}^3 a_{ji} + \frac{1}{f} \left(a_{j1} \text{KIE}_{\text{app}}^{13\text{C}} + a_{j2} \text{KIE}_{\text{app}}^{\text{D}} - a_{j1} - a_{j2}\right) = A_j + \frac{1}{f} K_j \left(\text{KIE}_{\text{app}}^{13\text{C}}, \text{KIE}_{\text{app}}^{\text{D}}\right) \quad (24)$$

For an analytical derivation of  $a^{\text{LS}}$  it is further assumed that the loss due to  $\text{O}(^1\text{D})$  can be neglected in the lower stratosphere. This is because  $\text{O}(^1\text{D})$  levels are low there (Fig. 5 of Bergamaschi et al., 1996). The CI fraction of  $a^{\text{LS}}$  is also small as will become apparent below, so that the additional lower stratospheric sink is primarily due to OH.

$$a_{2=\text{O}^1\text{D}}^{\text{LS}} = 0 \quad (25)$$

$$a_{1=\text{OH}}^{\text{LS}} = 1 - a_{3=\text{Cl}}^{\text{LS}}$$

This allows to further simplify the 2nd equation of Eq. (22) ( $j = 2$ , for  $a_{\text{O}^1\text{D}}$ ), using Eq. (24)

$$a_{2=\text{O}^1\text{D}}^{\text{G}} = x^{\text{US}} \cdot a_2^{\text{US}} = x^{\text{US}} \cdot \left(A_2 + \frac{1}{f} K_2\right) \quad (26)$$

**The isotopic composition of methane in the stratosphere**

T. Röckmann et al.

Title Page

Abstract

Introduction

Conclusions

References

Tables

Figures

⏪

⏩

◀

▶

Back

Close

Full Screen / Esc

Printer-friendly Version

Interactive Discussion



and to establish a relation between the stratospheric partitioning and the dynamical  $f$ -parameter

$$x^{\text{US}} = \frac{a_{\text{O}^1\text{D}}^{\text{G}}}{A_2 + \frac{1}{f}K_2} \quad (27)$$

This can be inserted in the 3rd equation of Eq. (22) ( $j = 3$ )

$$a_{3=\text{Cl}}^{\text{G}} = x^{\text{US}} \left( A_3 + \frac{1}{f}K_3 \right) + (1 - x^{\text{US}}) a_{\text{Cl}}^{\text{LS}} = a_{\text{Cl}}^{\text{LS}} + x^{\text{US}} \left( A_3 + \frac{1}{f}K_3 - a_{\text{Cl}}^{\text{LS}} \right) \quad (28)$$

Using Eq. (27) leads to

$$a_{\text{Cl}}^{\text{G}} - a_{\text{Cl}}^{\text{LS}} = x^{\text{US}} \frac{a_{\text{O}^1\text{D}}^{\text{G}}}{\left( A_2 + \frac{1}{f}K_2 \right)} \left( A_3 + \frac{1}{f}K_3 - a_{\text{Cl}}^{\text{LS}} \right) \quad (29)$$

and

$$f \left( A_2 \left( a_{\text{Cl}}^{\text{G}} - a_{\text{Cl}}^{\text{LS}} \right) - a_{\text{O}^1\text{D}}^{\text{G}} \left( A_3 - a_{\text{Cl}}^{\text{LS}} \right) \right) = a_{\text{O}^1\text{D}}^{\text{G}} K_3 - K_2 \left( a_{\text{Cl}}^{\text{G}} - a_{\text{Cl}}^{\text{LS}} \right). \quad (30)$$

This approach yields an equation for  $f$  as a function of  $a_{\text{Cl}}^{\text{LS}}$  and the apparent KIE measurements

$$f = \frac{K_3 a_{\text{O}^1\text{D}}^{\text{G}} - K_2 \left( a_{\text{Cl}}^{\text{G}} - a_{\text{Cl}}^{\text{LS}} \right)}{A_2 \left( a_{\text{Cl}}^{\text{G}} - a_{\text{Cl}}^{\text{LS}} \right) - a_{\text{O}^1\text{D}}^{\text{G}} \left( A_3 - a_{\text{Cl}}^{\text{LS}} \right)} = f \left( \text{KIE}_{\text{app}}^{^{13}\text{C}}, \text{KIE}_{\text{app}}^{\text{D}}, a_{\text{Cl}}^{\text{LS}} \right) \quad (31)$$

Inserting Eq. (31) back into (27) gives a similar expression for  $x^{\text{US}}$  and/or  $x^{\text{LS}}$

$$x^{\text{US}} = \frac{K_3 a_{\text{O}^1\text{D}}^{\text{G}} - K_2 \left( a_{\text{Cl}}^{\text{G}} - a_{\text{Cl}}^{\text{LS}} \right)}{K_3 A_2 - K_2 \left( A_3 - a_{\text{Cl}}^{\text{LS}} \right)} = x^{\text{US}} \left( \text{KIE}_{\text{app}}^{^{13}\text{C}}, \text{KIE}_{\text{app}}^{\text{D}}, a_{\text{Cl}}^{\text{LS}} \right) \quad (32)$$

**The isotopic composition of methane in the stratosphere**

T. Röckmann et al.

Title Page

Abstract

Introduction

Conclusions

References

Tables

Figures

⏪

⏩

◀

▶

Back

Close

Full Screen / Esc

Printer-friendly Version

Interactive Discussion



$$x^{\text{LS}} = 1 - x^{\text{US}} = x^{\text{LS}} \left( \text{KIE}_{\text{app}}^{13\text{C}}, \text{KIE}_{\text{app}}^{\text{D}}, a_{\text{Cl}}^{\text{LS}} \right) \quad (33)$$

The result of this approach of adding an additional lower stratospheric sink is that for each flight, we derive a single  $f$ -parameter for the middle and upper stratosphere (no  $\text{KIE}^{\text{D}}$ -discrimination), which can be compared to the value of 0.5 expected from the steady-state 1-D diffusive model and allows to calculate a sink partitioning for the middle and upper stratosphere. We furthermore obtain an estimate for the loss fraction in the lower stratosphere, which can be compared to additional measurements/independent calculations (see Appendix A). Both parameters depend on the Cl-sink strength in the LS (Eq. 25), which in principle could reversely be confined from the choice of reasonable intervals of  $f$  and/or  $x^{\text{US}}$ .

Values of the sink partitioning with an additional pure OH sink, i.e., for  $a_{\text{Cl}} = 0$ , are shown in Table 8. A nice result is that compared to Table 6 (single mean global sink partitioning) the values for  $f$  are shifted closer to 0.5. By definition, there is no  $\text{KIE}^{\text{D}}$ -discrimination ( $f_r = 1$ ). For the mid-litudinal and the non-vortex profiles  $f$ -values are in tendency slightly larger than 0.5 ( $\pm 0.02$ ), the subtropical  $f$  is slightly lower ( $f \sim 0.47$ ) and for vortex profiles the  $f$ -value varies between 0.43–0.48. The values below 0.5 might reflect the higher dynamic interaction leading to an increased degree of mixing in these regions (e.g. recirculation in the tropics, vortex breakup at high latitudes). This is supported by the decreasing  $f$  values for the three KIR-92 flights in the period of vortex breakup.

The lower sink fraction  $x^{\text{LS}}$  increases towards high latitudes because of the lower  $\delta\text{D}$  values of vortex air. In the global sink partitioning following Eq. (10) the  $\text{O}(^1\text{D})$  sink fraction is increased at the cost of the OH sink leading to a decrease in  $f_r$ . As  $f_r$  is forced to unity here, the effect is ascribed to the additional lower stratospheric sink,  $x^{\text{LS}}$ , which has to be larger. The values for  $f$  depend on the assumed value of  $a^{\text{LS}}(\text{Cl})$ . Already a chlorine sink fraction of 5% in the lower stratosphere lifts all derived  $f$ -values above 0.5 and thus brings them again into agreement with the 1-D-diffusive model

## The isotopic composition of methane in the stratosphere

T. Röckmann et al.

Title Page

Abstract

Introduction

Conclusions

References

Tables

Figures

⏪

⏩

◀

▶

Back

Close

Full Screen / Esc

Printer-friendly Version

Interactive Discussion



expectations. It is important to recall that the absolute values depend on the assumed (modelled) mean global sink partitioning and thus, rely on the correctness of the model calculation.

In summary, the assumption of an additional OH-dominated sink, located in the lower stratosphere and/or tropopause region allows correcting for the KIE<sup>D</sup>-discrimination and calculating a reasonable sink partitioning for the middle/upper stratospheric sink. The additional lower sink fraction that has to be added to force  $f^r = 1$  is 20 to 30%. Under these conditions,  $f$ -values are shifted closer to expectations ( $f \sim 0.5$ ). If  $x^{\text{LS}}$  is chosen smaller, then the inferred  $f$ -parameter increases.  $f$  also increases if only a small contribution of Cl to the lower stratospheric sink is assumed.

## 8 Mesosphere-stratosphere exchange in the vortex

It was already discussed above that the isotope:isotope correlation is different for mid-latitude and vortex samples (Fig. 3). The correlation for the mid latitudes is practically linear. The correlation for the vortex samples becomes more flat, i.e., it has a lower  $\delta\text{D}$  for a given  $\delta^{13}\text{C}$  value. Based on the KIE values in Table 1 this can be tentatively attributed to stronger removal by O(<sup>1</sup>D) for the vortex samples, as these have descended from high altitudes where removal by O(<sup>1</sup>D) is expected to be more effective. The vortex region is generally characterized by subsidence of air from higher altitudes in the stratosphere and additionally mesospheric air can subside into the stratospheric polar vortex. For flight KIR-03-03, this has been investigated in detail in Engel et al. (2006), and it is interesting to note that the samples that were characterized there as having mesospheric influence do not show unusual behaviour in our correlations. This suggests that the influence of mesospheric air on CH<sub>4</sub> in the vortex is not an exception in 2003 as it looks in the individual profiles, but that the descent of mesospheric air causes a general deviation of the isotope-isotope correlation in the vortex from the one at mid latitudes.

### The isotopic composition of methane in the stratosphere

T. Röckmann et al.

Title Page

Abstract

Introduction

Conclusions

References

Tables

Figures

⏪

⏩

◀

▶

Back

Close

Full Screen / Esc

Printer-friendly Version

Interactive Discussion



## The isotopic composition of methane in the stratosphere

T. Röckmann et al.

Title Page

Abstract

Introduction

Conclusions

References

Tables

Figures

⏪

⏩

◀

▶

Back

Close

Full Screen / Esc

Printer-friendly Version

Interactive Discussion



Surprisingly, the sample right below the mesospheric intrusion (KIR-03-03/12) deviates from this general classification. In Table 10 this sample is compared to sample KIR-03-03/6, which is the most enriched sample of the vortex branch of the isotope-isotope correlation, and clearly influenced by mesospheric air (Engel et al., 2006). Although KIR-03-03/06 contains less methane than KIR-03-03/12, i.e., it has undergone more methane removal, it is less enriched. This can be explained if KIR-03-03/12 has been processed more strongly by sink process with strong KIE, namely Cl. We propose that sample KIR-03-03/12, represents air that originates from the upper stratosphere, likely close to the stratopause, and from outside the vortex, which descends to the middle and lower stratosphere below the mesospheric intrusion.

Based on the previous results of this mesospheric air discussed in Engel et al. (2006) and the specific position of KIR-03-03/12 between the two characteristic lines in the isotope-isotope plot (Fig. 12), it can be assumed that KIR-03-03/12 itself is a result of an end-member mixing between the most enriched air sample on the vortex branch, i.e. KIR-03-03/6, and a suitable (unknown) end-member from the upper stratosphere, denoted KIR-03-03/US. As the products of mixing are found on a straight line connecting the two end-members, the unknown upper stratospheric member must also fall on an extrapolated line through KIR-03-03/6 (on the vortex branch) and KIR-03-03/12. We can further assume that KIR-03-03/US falls on the extrapolation of the mid-latitude isotope-isotope correlation (compare Fig. 12). The intersection then defines the isotopic composition of KIR-03-03/US under the given assumptions as given in Table 10. In this case, it is also straightforward to determine the relative contributions of the two end-members as 45.5% of KIR-03-03/US and 54.5% of KIR-03-03/6.

## 9 Conclusions

Measurements of the  $^{13}\text{C}$  and D content of  $\text{CH}_4$  on a large set of stratospheric air samples collected over a period of 16 yr provide the most comprehensive picture so far on the isotopic composition of stratospheric  $\text{CH}_4$ . A method to take into account the residence time in the stratosphere in combination with the observed mixing ratio and

isotope trends in the troposphere has been presented. The highest isotope enrichments are found in the polar vortex with values up to  $\delta^{13}\text{C} = -19\text{‰}$  and  $\delta\text{D} = +190\text{‰}$ , strongly extending the range of isotope enrichments observed before. The previously available isotope data from different laboratories and on air samples collected at different locations and times can be linked and compared by relating them to the new large dataset. It also becomes apparent that inter-laboratory differences exist, especially for  $\delta\text{D}$ .

In addition to the three chemical sink processes, mixing processes have a strong influence on the isotopic composition of stratospheric  $\text{CH}_4$ . When trace gases are mixed across a dynamical barrier, like the polar vortex, the resulting effect on the apparent fractionation constant can be even larger than what is expected from diffusive mixing only.

It has been shown that care has to be taken when mean kinetic isotope effects derived from single balloon profiles are compared. Due to the non-linearity of the isotope-mixing ratio relation in a Rayleigh fractionation plot the samples at the lowest mixing ratio have the strongest leverage on the overall slope. Therefore, only profiles that cover the same range of mixing ratios should be compared directly. If profiles from different times are compared, the temporal mixing ratio and isotope trends also need to be taken into account.

Isotope-isotope correlations show that samples from the polar vortex are less depleted in  $\delta\text{D}$  than at mid-latitudes, which is attributed to enhanced chemical destruction by  $\text{O}(^1\text{D})$  for the vortex samples. A detailed analysis of methods to derive a sink partitioning from global mean kinetic isotope effects is carried out. The classical formal sink partitioning, which is based on the assumption that all sinks act simultaneously, underestimates the contribution from OH, because the KIE values derived in the stratosphere are less influenced by the removal in the lower stratosphere compared to the upper stratosphere. Therefore, global models that include the isotopic composition are needed to derive a reliable sink partitioning from the measurements, similar to the study by McCarthy et al. (2003).

## The isotopic composition of methane in the stratosphere

T. Röckmann et al.

[Title Page](#)[Abstract](#)[Introduction](#)[Conclusions](#)[References](#)[Tables](#)[Figures](#)[⏪](#)[⏩](#)[◀](#)[▶](#)[Back](#)[Close](#)[Full Screen / Esc](#)[Printer-friendly Version](#)[Interactive Discussion](#)

### Independent estimate of the lower sink fraction

The CH<sub>4</sub> loss rate in the stratosphere can be independently inferred from the inverse of the  $\Gamma_{\text{CH}_4}(c)$  relation (Fig. 13a), as  $c(\Gamma)$  describes a temporal development of the methane mixing ratio. The first derivative  $c'(\Gamma)$  expresses a rate of change of the CH<sub>4</sub> mixing ratio (Fig. 13b), which is used as an estimate for the methane loss rate  $L_{\text{est}}$ . More exactly, only the change of this relation at a certain mixing ratio level relative to the loss over the whole mixing ratio range is used.

Similar to  $\Gamma_{\text{CH}_4}$  the derivation is derived from a spline-fit, which was then approximated piecewise by polynomials (see Table 9).

$$L_{\text{est}}(c) = A_4c^4 + A_3c^3 + A_2c^2 + A_1c + A_0 \quad (\text{A1})$$

Integrating Eq. (A1) over the whole range of mixing ratios neglects the different absolute contribution in each  $c$ -interval. In total there is more methane (and air molecules) at lower altitudes, where the pressure is higher than in the upper stratosphere (even if the mixing ratio at both points would be equal).

A suitable weighting function is given by the particle number derived from the ideal gas equation

$$n(z) = \frac{p(z)V(z)}{R_m T} = \frac{4\pi}{R_m T} p(z)(z + R_E)^2 \Delta z \quad (\text{A2})$$

where  $z$  denotes the altitude above earth surface,  $R_E = 6371.2$  km is the mean earth radius and  $R_m = 8.3145$  J/(mol K)<sup>-1</sup> is the molar gas constant.  $p(z)$  for the range observed altitude range (above 12 km) is determined from mid-latitudinal and non-vortex flights (ASA-01-10, ASA-02-09, KIR-03-06)

$$p(z) = p_0 e^{-bz} = 1193.7 e^{-0.1530z} \quad (\text{A3})$$

### The isotopic composition of methane in the stratosphere

T. Röckmann et al.

Title Page

Abstract

Introduction

Conclusions

References

Tables

Figures

⏪

⏩

◀

▶

Back

Close

Full Screen / Esc

Printer-friendly Version

Interactive Discussion



The integration of Eq. (A2) from  $z_1 = 16.2$  km ( $p(z_1) \sim 100$  mb) to  $z_2 \sim 48$  km, for a constant stratospheric temperature of  $T_{\text{strat}} \sim T = 223$  K yields  $18.2 \times 10^{+6}$  Tmol and after multiplying with the mean molar weight of air  $M_{\text{air}} = 28.96$  u, this corresponds to a total mass  $5.28 \times 10^8$  Tg, which is in reasonable agreement with the total stratospheric mass above the 100 mb layer of  $5.2 \times 10^8$  Tg stated in Holton (1990) and similar numbers in textbooks.

To integrate  $L_{\text{est}}(c)$  in Eq. (A1) with the weight  $n(z)$ , a parameter substitution, here  $z(c)$ , was derived from mid-latitudinal/non-vortex flights

$$z(c) = -5.8 \cdot c^3 + 15.8 \cdot c^2 - 31.3 \cdot c + 48.2 \text{ [in km]}$$

$$\frac{dz}{dc} = -17.4 \cdot c^2 + 31.5 \cdot c - 31.3 \quad (\text{A4})$$

The integration is done numerically with a step size of  $\Delta c = -0.01$  ppm ( $\Delta z \sim 180\text{--}350$  m) and the normalization constant  $L$  for the estimated loss rate is calculated by

$$L = \sum_{c_i=1.78}^{0.25} \frac{L_{\text{est}}(z(c_i))}{L} p(z(c_i)) z(c_i)^2 \left( \frac{dz}{dc} \right)_{c_i} \Delta c \quad (\text{A5})$$

The relative estimated loss rate is shown in Fig. 13c. The relative loss fraction observed in the lower stratosphere until a mixing ratio of 1650 mb

$$x_{\text{est}} = \sum_{c_i=1.78}^{1.65} \frac{L_{\text{est}}(z(c_i))}{L} p(z(c_i)) z(c_i)^2 \left( \frac{dz}{dc} \right)_{c_i} \Delta c \quad (\text{A6})$$

is  $x_{\text{est}} = 18.5\%$ . This number has to be seen as lower limit since the above derivation neglects stratosphere-troposphere exchange, which due to the stable tropospheric input with comparably high mixing ratio leads to a less pronounced rate of change rate than expected from the chemical loss alone. The final estimate depends on the chosen mixing ratio cut-off (28% at 1550 ppb and 24% at 1600 ppb). In Eq. (A6) a cut-off of  $c = 1.65$  was selected, which roughly marks the edge of the rather stable KIE region.

## The isotopic composition of methane in the stratosphere

T. Röckmann et al.

Title Page

Abstract

Introduction

Conclusions

References

Tables

Figures

⏪

⏩

◀

▶

Back

Close

Full Screen / Esc

Printer-friendly Version

Interactive Discussion



Thus, the amount of CH<sub>4</sub> removed in the lower stratosphere (mostly by OH) is similar to the additional lower stratospheric sink introduced in Sect. 7.3. Although this comparison remains qualitative only, it provides independent support for the estimates on  $x^{\text{LS}}$  derived there.

5 *Acknowledgements.* This project was funded by the German BmBF in the AFO 2000 program, (project ISOSTRAT) and the Dutch NWO (grant number 865.07.001).

## References

10 Andrews, A. E., Boering, K. A., Wofsy, S. C., Daube, B. C., Jones, D. B., Alex, S., Loewenstein, M., Podolske, J. R., and Strahan, S. E.: Empirical age spectra for the midlatitude lower stratosphere from in situ observations of CO<sub>2</sub>: Quantitative evidence for a subtropical “barrier” to horizontal transport, *J. Geophys. Res.*, 106, 10257–10274, 2001.

Andrews, D. G., Holton, J. R., and Leovy, C. B.: *Middle Atmosphere Dynamics*, Academic Press, 1987.

15 Avallone, L. M. and Prather, M. J.: Photochemical evolution of ozone in the lower tropical stratosphere, *J. Geophys. Res.*, 101, 1457–1461, 1996.

Bergamaschi, P., Brühl, C., Brenninkmeijer, C. A. M., Saueressig, G., Crowley, J. N., Grooss, J. U., Fischer, H., and Crutzen, P. J.: Implications of the large carbon kinetic isotope effect in the reaction CH<sub>4</sub>+Cl for the <sup>13</sup>C/<sup>12</sup>C ratio of stratospheric CH<sub>4</sub>, *Geophys. Res. Lett.*, 23, 2227–2230, 1996.

20 Bergamaschi, P., Brenninkmeijer, C. A. M., Hahn, M., Röckmann, T., Scharffe, D. H., Crutzen, P. J., Elansky, N. F., Belikov, I. B., Trivett, N. B. A., and Worthy, D. E. J.: Isotope analysis based source identification for atmospheric CH<sub>4</sub> and CO across Russia using the Trans-Siberian railroad, *J. Geophys. Res.*, 103(D7), 8227–8235, 1998.

25 Bergamaschi, P., Bräunlich, M., Marik, T., and Brenninkmeijer, C. A. M.: Measurements of the carbon and hydrogen isotopes of atmospheric methane at Izana, Tenerife: Seasonal cycles and synoptic-scale variations, *J. Geophys. Res.*, 105, 14531–14546, 2000.

Bergamaschi, P., Lowe, D. C., Manning, M. R., Moss, R., Bromley, T., and Clarkson, T. S.: Transsects of atmospheric CO, CH<sub>4</sub>, and their isotopic composition across the Pacific: Shipboard measurements and validation of inverse models, *J. Geophys. Res.*, 106, 7993–8011, 2001.

## The isotopic composition of methane in the stratosphere

T. Röckmann et al.

Title Page

Abstract

Introduction

Conclusions

References

Tables

Figures

⏪

⏩

◀

▶

Back

Close

Full Screen / Esc

Printer-friendly Version

Interactive Discussion



**The isotopic composition of methane in the stratosphere**

T. Röckmann et al.

[Title Page](#)[Abstract](#)[Introduction](#)[Conclusions](#)[References](#)[Tables](#)[Figures](#)[⏪](#)[⏩](#)[◀](#)[▶](#)[Back](#)[Close](#)[Full Screen / Esc](#)[Printer-friendly Version](#)[Interactive Discussion](#)

Boering, K. A., Wofsy, S. C., Daube, B. C., Schneider, H. R., Loewenstein, M., and Podolske, J. R.: Stratospheric mean ages and transport rates from observations of carbon dioxide and nitrous oxide, *Science*, 274, 1340–1343, 1996.

Brass, M. and Röckmann, T.: Continuous-flow isotope ratio mass spectrometry method for carbon and hydrogen isotope measurements on atmospheric methane, *Atmos. Meas. Tech.*, 3, 1707–1721, doi:10.5194/amt-3-1707-2010, 2010.

Brenninkmeijer, C. A. M., Lowe, D. C., Manning, M. R., Sparks, R. J., and Velthoven, P. F. J. v.: The  $^{13}\text{C}$ ,  $^{14}\text{C}$ , and  $^{18}\text{O}$  isotopic composition of  $\text{CO}$ ,  $\text{CH}_4$  and  $\text{CO}_2$  in the higher southern latitudes lower stratosphere, *J. Geophys. Res.*, 100, 26163–26172, 1995.

Brenninkmeijer, C. A. M., Müller, R., Crutzen, P. J., Lowe, D. C., Manning, M. R., Sparks, R. J., and Velthoven, P. J. v.: A large  $^{13}\text{C}$  deficit in the lower Antarctic stratosphere due to “ozone hole” chemistry: Part 1, observations, *Geophys. Res. Lett.*, 23, 2125–2128, 1996.

Brewer, A. W.: Evidence for a World Circulation Provided by the Measurements of Helium and Water Vapour Distribution in the Stratosphere, *Q. J. Roy. Meteorol. Soc.*, 75, 351–363, 1949.

Dlugokencky, E. J., Masarie, K. A., Lang, P. M., and Tans, P. P.: Continuing decline in the growth rate of the atmospheric methane burden, *Nature*, 393, 447–450, 1998.

Dobson, G. M. B., Brewer, A. W., and Cwilong, B. M.: Meteorology of the Lower Stratosphere, *P. Roy. Soc London Ser-A*, 185, 144–175, 1946.

Engel, A., Möbius, T., Haase, H.-P., Bönisch, H., Wetter, T., Schmidt, U., Levin, I., Reddman, T., Oelhaf, H., Wetzell, G., Grunow, K., Huret, N., and Pirre, M.: Observation of mesospheric air inside the arctic stratospheric polar vortex in early 2003, *Atmos. Chem. Phys.*, 6, 267–282, doi:10.5194/acp-6-267-2006, 2006.

Erikson, E.: Deuterium and oxygen-18 in precipitation and other natural waters: Some theoretical considerations, *Tellus*, 17, 498–512, 1965.

Gupta, M., Tyler, S., and Cicerone, R.: Modeling atmospheric  $\delta^{13}\text{C}$  and the causes of recent changes in atmospheric  $\text{CH}_4$  amounts, *J. Geophys. Res.*, 101, 22923–22932, 1996.

Hall, T. M. and Plumb, R. A.: Age as a Diagnostic of Stratospheric Transport, *J. Geophys. Res.*, 99, 1059–1070, 1994.

Holton, J. R.: A dynamically based transport parameterization for one-dimensional photochemical models of the stratosphere, *J. Geophys. Res.*, 91(D2), 2681–2686, doi:10.1029/JD091iD02p02681, 1986.

Holton, J. R.: On the Global Exchange of Mass between the Stratosphere and Troposphere, *J. Atmos. Sci.*, 47, 392–395, 1990.

## The isotopic composition of methane in the stratosphere

T. Röckmann et al.

Title Page

Abstract

Introduction

Conclusions

References

Tables

Figures

◀

▶

◀

▶

Back

Close

Full Screen / Esc

Printer-friendly Version

Interactive Discussion

- Holton, J. R., Haynes, P. H., McIntyre, M. E., Douglas, A. R., Rood, R. B., and Pfister, L.: Stratosphere-Troposphere Exchange, *Rev. Geophys.*, 33, 403–439, 1995.
- Irion, F. W., Moyer, E. J., Gunson, M. R., Rinsland, C. P., Yung, Y. L., Michelsen, H. A., Salawitch, R. J., Chang, A. Y., Newchurch, M. J., Abbas, M. M., Abrams, M. C., and Zander, R.: Stratospheric observations of CH<sub>3</sub>D and HDO from ATMOS infrared solar spectra: Enrichments of deuterium in methane and implications for HD, *Geophys. Res. Lett.*, 23, 2381–2384, 1996.
- Kaiser, J., Brenninkmeijer, C. A. M., and Röckmann, T.: Intramolecular <sup>15</sup>N and <sup>18</sup>O fractionation in the reaction of N<sub>2</sub>O with O(<sup>1</sup>D) and its implications for the stratospheric N<sub>2</sub>O isotope signature, *J. Geophys. Res.*, 107, 4214, doi:10.1029/2001JD001506, 2002.
- Kaiser, J., Engel, A., Borchers, R., and Röckmann, T.: Probing stratospheric transport and chemistry with new balloon and aircraft observations of the meridional and vertical N<sub>2</sub>O isotope distribution, *Atmos. Chem. Phys.*, 6, 3535–3556, doi:10.5194/acp-6-3535-2006, 2006.
- Kaye, J. A.: Mechanisms and Observations for Isotope Fractionation of Molecular-Species in Planetary-Atmospheres, *Rev. Geophys.*, 25, 1609–1658, 1987.
- Kida, H.: General-circulation of air parcels and transport characteristics derived from a hemispheric GCM, 2. Very long-term motions of air parcels in the troposphere and stratosphere, *J. Meteorol. Soc. Jap.*, 61, 510–522, 1983.
- Lowe, D. C., Manning, M. R., Brailsford, G. W., and Bromley, A. M.: The 1991–1992 atmospheric methane anomaly: Southern Hemisphere C-13 decrease and growth rate fluctuations, *Geophys. Res. Lett.*, 24, 857–860, 1997.
- Mahlman, J. D., Levy II, H., and Moxim, W. J.: Three-dimensional simulations of stratospheric N<sub>2</sub>O: Predictions for other trace constituents., *J. Geophys. Res.*, 91, 2687–2707. (Correction, *J. Geophys. Res.*, 2691, 9921, doi:10.1029/JD091iD02p02687, 1986.
- McCarthy, M. C., Connell, P., and Boering, K. A.: Isotopic fractionation of methane in the stratosphere and its effect on free tropospheric isotopic compositions, *Geophys. Res. Lett.*, 28, 3657–3660, 2001.
- McCarthy, M. C., Boering, K. A., Rice, A. L., Tyler, S. C., Connell, P., and Atlas, E.: Carbon and hydrogen isotopic compositions of stratospheric methane: 2. Two-dimensional model results and implications for kinetic isotope effects, *J. Geophys. Res.*, 108, 4461, doi:10.1029/2002JD003183, 2003.
- McIntyre, M. E. and Palmer, T. N.: Breaking planetary waves in the stratosphere, *Nature*, 305, 593–600, 1983.

**The isotopic composition of methane in the stratosphere**

T. Röckmann et al.

[Title Page](#)[Abstract](#)[Introduction](#)[Conclusions](#)[References](#)[Tables](#)[Figures](#)[⏪](#)[⏩](#)[◀](#)[▶](#)[Back](#)[Close](#)[Full Screen / Esc](#)[Printer-friendly Version](#)[Interactive Discussion](#)

Michelsen, H. A., Manney, G. L., Gunson, M. R., Rinsland, C. P., and Zander, R.: Correlations of stratospheric abundances of CH<sub>4</sub> and N<sub>2</sub>O derived from ATMOS measurements, *Geophys. Res. Lett.*, 25, 2777–2780, 1998.

5 Miller, J. B., Mack, K. A., Dissly, R., White, J. W. C., Dlugokencky, E. J., and Tans, P. P.: Development of analytical methods and measurements of <sup>13</sup>C/<sup>12</sup>C in atmospheric CH<sub>4</sub> from the NOAA/CMDL global air sampling network, *J. Geophys. Res.*, 107, 4178, doi:4110.1029/2001JD000630, 2002.

Neu, J. L. and Plumb, R. A.: Age of air in a "leaky pipe" model of stratospheric transport, *J. Geophys. Res.*, 104, 19243–19255, 1999.

10 Plumb, R. A. and Ko, M. K. W.: Interrelationships between Mixing Ratios of Long Lived Stratospheric Constituents, *J. Geophys. Res.*, 97, 10145–10156, 1992.

Plumb, R. A.: A "tropical pipe" model of stratospheric transport, *J. Geophys. Res.*, 101, 3957–3972, 1996.

15 Plumb, R. A., Waugh, D. W., and Chipperfield, M. P.: The effects of mixing on traces relationships in the polar vortices, *J. Geophys. Res.*, 105, 10047–10062, 2000.

Quay, P., Stutsman, J., Wilbur, D., Snover, A., Dlugokencky, E., and Brown, T.: The isotopic composition of atmospheric methane, *Global Biogeochem. Cy.*, 13, 445–461, 1999.

Rahn, T., Zhang, H., Wahlen, M., and Blake, G. A.: Stable isotope fractionation during ultraviolet photolysis of N<sub>2</sub>O, *Geophys. Res. Lett.*, 25, 4489–4492, 1998.

20 Rice, A. L., Gotoh, A. A., Ajie, H. O., and Tyler, S. C.: High-precision continuous-flow measurement of δ<sup>13</sup>C and δD of atmospheric CH<sub>4</sub>, *Anal. Chem.*, 73, 4104–4110, 2001.

Rice, A. L., Tyler, S. C., McCarthy, M. C., Boering, K. A., and Atlas, E.: Carbon and hydrogen isotopic compositions of stratospheric methane: 1. High-precision observations from the NASA ER-2 aircraft, *J. Geophys. Res.*, 108(D15), 4460, doi:10.1029/2002JD003042, 2003.

25 Ridal, M. and Siskind, D. E.: A two-dimensional simulation of the isotopic composition of water vapor and methane in the upper atmosphere, *J. Geophys. Res.*, 107, 4807, doi:4810.1029/2002JD002215, 2002.

Saueressig, G., Bergamaschi, P., Crowley, J. N., Fischer, H., and Harris, G. W.: Carbon kinetic isotope effect in the reaction of CH<sub>4</sub> with Cl atoms, *Geophys. Res. Lett.*, 22, 1225–1228, 1995.

30 Saueressig, G., Bergamaschi, P., Crowley, J. N., Fischer, H., and Harris, G. W.: D/H kinetic isotope effect in the reaction CH<sub>4</sub> + Cl, *Geophys. Res. Lett.*, 23, 3619–3622, 1996.

Saueressig, G., Crowley, J. N., Bergamaschi, P., Brühl, C., Brenninkmeijer, C. A. M., and Fis-

**The isotopic composition of methane in the stratosphere**

T. Röckmann et al.

[Title Page](#)[Abstract](#)[Introduction](#)[Conclusions](#)[References](#)[Tables](#)[Figures](#)[⏪](#)[⏩](#)[◀](#)[▶](#)[Back](#)[Close](#)[Full Screen / Esc](#)[Printer-friendly Version](#)[Interactive Discussion](#)

cher, H.: Carbon 13 and D kinetic isotope effects in the reactions of CH<sub>4</sub> with O(<sup>1</sup>D) and OH: New laboratory measurements and their implications for the isotopic composition of stratospheric methane, *J. Geophys. Res.*, 106, 23127–23138, 2001.

Schmidt, U., Kulassa, G., Klein, E., Roth, E. P., Fabian, P., and Borchers, R.: Intercomparison of Balloon-Borne Cryogenic Whole Air Samplers During the Map-Globus 1983 Campaign, *Planet. Space Sci.*, 35, 647–656, 1987.

Simpson, I. J., Blake, D. R., Rowland, F. S., and Chen, T. Y.: Implications of the recent fluctuations in the growth rate of tropospheric methane, *Geophys. Res. Lett.*, 29, 1479, doi:10.1029/2001GL014521, 2002.

Stevens, C. M. and Rust, F. E.: The Carbon Isotopic Composition of Atmospheric Methane, *J. Geophys. Res.*, 87, 4879–4882, 1982.

Sugawara, S., Nakazawa, T., Shirakawa, Y., Kawamura, K., and Aoki, S.: Vertical profile of the carbon isotopic ratio of stratospheric methane over Japan, *Geophys. Res. Lett.*, 24, 2989–2992, 1997.

Tarasova, O. A., Brenninkmeijer, C. A. M., Assonov, S. S., Elansky, N. F., Röckmann, T., and Brass, M.: Atmospheric CH<sub>4</sub> along the Trans-Siberian railroad (TROICA) and river Ob: Source identification using stable isotope analysis, *Atmos. Environ.*, 40, 5617–5628, 2006.

Tyler, S. C., Ajie, H. O., Gupta, M. L., Cicerone, R. J., Blake, D. R., and Dlugokencky, E. J.: Stable carbon isotopic composition of atmospheric methane: A comparison of surface level and free tropospheric air, *J. Geophys. Res.*, 104, 13895–13910, 1999.

Volk, C. M., Elkins, J. W., Fahey, D. W., Dutton, G. S., Gilligan, J. M., Loewenstein, M., Podolske, J. R., Chan, K. R., and Gunson, M. R.: Quantifying transport between the tropical and mid-latitude lower stratosphere, *Science*, 272, 1763–1768, 1996.

Wahlen, M.: The Global Methane Cycle, *Annu. Rev. Earth Planet. Sci.*, 21, 407–426, 1993.

Wahlen, M., Tanaka, N., Henty, R., Deck, B., Zeglen, J., Vogel, J. S., Southon, J., Shemesh, A., Fairbanks, R., and Broecker, W.: Carbon-14 in Methane Sources and in Atmospheric Methane: The Contribution from Fossil Carbon, *Science*, 245, 286–290, 1989.

Wang, J. S., McElroy, M. B., Spivakovsky, C. M., and Jones, D. B. A.: On the contribution of anthropogenic Cl to the increase in  $\delta^{13}\text{C}$  of atmospheric methane, *Global Biogeochem. Cy.*, 16, 1047, doi:10.1029/2001GB001572, 2002.

Waugh, D. W. and Rong, P. P.: Interannual variability in the decay of lower stratospheric Arctic vortices, *J. Meteorol. Soc. Japan*, 80, 997–1012, 2002.

Waugh, D. W., Plumb, R. A., Elkins, J. W., Fahey, D. W., Boering, K. A., Dutton, G. S., Volk,

C. M., Keim, E., Gao, R. S., Daube, B. C., Wofsy, S. C., Loewenstein, M., Podolske, J. R., Chan, K. R., Proffitt, M. H., Kelly, K., Newman, P. A., and Lait, L. R.: Mixing of polar vortex air into middle latitudes as revealed by tracer-tracer scatterplots, *J. Geophys. Res.*, 102, 13119–13134, 1997.

- 5 WMO: (World Meteorological Organization), Scientific Assessment of Ozone Depletion: 2002, Global Ozone Research and Monitoring Project, Report Nr 47, Geneva, 498 pp., 2003.

---

**The isotopic composition of methane in the stratosphere**

T. Röckmann et al.

---

Title Page

Abstract

Introduction

Conclusions

References

Tables

Figures



Back

Close

Full Screen / Esc

Printer-friendly Version

Interactive Discussion



## The isotopic composition of methane in the stratosphere

T. Röckmann et al.

**Table 1.** Measured and calculated kinetic isotope effects and coefficients for their temperature dependence  $KIE(T) = A \exp(B/T)$ .

	$KIE^{13C}(T = 296 \text{ K})$	$T$	$A$	$B$	$KIE^{13C}(T = 223 \text{ K})$		
OH	$1.0039 \pm 0.0004$		?	?			Saueressig et al. (2001)
O( <sup>1</sup> D)	1.013	223–295		0	1.013	meas.	Saueressig et al. (2001)
Cl	$1.066 \pm 0.02$	223–297	1.043	6.455	$1.075 \pm 0.005$	meas.	Saueressig et al. (1995)
	$KIE^D$			$KIE^D$			
OH	$1.294 \pm 0.018$		1.097*	$49 \pm 22$	1.367	calc.	Saueressig et al. (2001)
O( <sup>1</sup> D)	$1.066 \pm 0.002$	224–295		0	1.06	meas.	Saueressig et al. (2001)
Cl	$1.508 \pm 0.04$	223–295	1.278	$51.31 \pm 19.1$	1.61	meas.	Saueressig et al. (1996)

\* Adjusted T-dependence from [Gierczak97] to match room temperature measurement.

[Title Page](#)
[Abstract](#)
[Introduction](#)
[Conclusions](#)
[References](#)
[Tables](#)
[Figures](#)
[Back](#)
[Close](#)
[Full Screen / Esc](#)
[Printer-friendly Version](#)
[Interactive Discussion](#)


## The isotopic composition of methane in the stratosphere

T. Röckmann et al.

Title Page

Abstract

Introduction

Conclusions

References

Tables

Figures

⏪

⏩

◀

▶

Back

Close

Full Screen / Esc

Printer-friendly Version

Interactive Discussion



**Table 2.** Overview of balloon flights and number of samples analyzed for  $\delta^{13}\text{C}$  and  $\delta\text{D}$  (column  $^{13}\text{C}$  and D). Each flight is given a flight ID as STA-JJ-MM, where STA is the 3-letter-code for the balloon launch station, JJ the year and MM the month of sampling.

Flight ID	Flight date	Location	$^{13}\text{C}$	D	Characteristics
Flights operated by MPI für Sonnensystemforschung					
HYD-87-03	03/26/87	HYD <sup>1</sup>	5	5	Subtropical
KIR-92-01	01/18/92	KIR <sup>2</sup>	13	13	Arctic weak vortex, final warming series
KIR-92-02	02/06/92	KIR <sup>2</sup>	10	10	final warming series
KIR-92-03	03/20/92	KIR <sup>2</sup>	10	9	final warming series
ASA-93-09	09/30/93	ASA <sup>3</sup>	15	15	mid-latitude background
KIR-95-03	03/07/95	KIR <sup>2</sup>	11	11	Arctic with mid-latitude characteristics
HYD-99-04	04/29/99	HYD <sup>1</sup>	10	9	Subtropical
GAP-99-06	06/23/99	GAP <sup>4</sup>	15	15	mid-latitude summer
Flights operated by Institut für Meteorologie und Geophysik, Universität Frankfurt					
KIR-00-01	01/03/00	KIR <sup>2</sup>	13	– <sup>5</sup>	Arctic strong vortex
ASA-01-10	10/11/01	ASA <sup>3</sup>	13	– <sup>5</sup>	mid-latitude background
ASA-02-09	09/15/02	ASA <sup>3</sup>	13	6	mid-latitude background
KIR-03-03	03/06/03	KIR <sup>2</sup>	13	13	Arctic vortex, mesospheric enclosure
KIR-03-06	06/09/03	KIR <sup>2</sup>	13	13	Arctic summer

<sup>1</sup> HYD: Hyderabad, India (17.5° N, 78.60° E);

<sup>2</sup> KIR: Kiruna, Sweden (67.9° N, 21.10° E);

<sup>3</sup> ASA: Aire sur l'Adour, France (43.70° N, –0.30° E);

<sup>4</sup> GAP: Gap, France (44.44° N, 6.14° E);

<sup>5</sup>  $\delta\text{D}$  analyses not fully developed at that time.

## The isotopic composition of methane in the stratosphere

T. Röckmann et al.

Title Page

Abstract

Introduction

Conclusions

References

Tables

Figures

◀

▶

◀

▶

Back

Close

Full Screen / Esc

Printer-friendly Version

Interactive Discussion



**Table 3.** Mean KIE per flight, in brackets error on last digits. Additionally the column “ $c_{\min}$ ” shows the minimal mixing ratio in a sample set used to derive the corresponding mean KIE.

Sample set	KIE $^{13}\text{C}$	$r^2$	Excluded samples	$c_{\min}$ ppb	KIE <sup>D</sup>	$r^2$	Excluded samples	$c_{\min}$ ppb
KIR-92-01	1.0162 (3)	0.996		265	1.142 (1)	0.999	8,9	335
KIR-92-02	1.0157 (3)	0.997		272	1.129 (2)	0.999		272
KIR-92-03	1.0144 (3)	0.996		397	1.128 (3)	0.997		397
KIR-00-01	1.0170 (2)	0.999		248				
KIR-03-03	1.0168 (3)	0.998	1,12	271	1.133 (5)	0.991	12	271
<b>average (vortex)</b>	<b>1.0160 (10)</b>				<b>1.133 (6)</b>			
KIR-03-06	1.0168 (5)	0.991		652	1.147 (4)	0.993		652
KIR-95-03	1.0148 (4)	0.995		835	1.150 (3)	0.998		835
<b>average (non-vortex)</b>	<b>1.0158 (14)</b>				<b>1.146(0.5)</b>			
<b>average (all polar)</b>	<b>1.0159 (9)</b>				<b>1.138 (8)</b>			
ASA-93-09	1.0153 (5)	0.989	7	831	1.160 (6)	0.984		613
GAP-99-06	1.0165 (4)	0.993		631	1.153 (3)	0.997		631
ASA-01-10	1.0153 (2)	0.998		957				
ASA-02-09	1.0151 (5)	0.989		897	1.140 (21)	0.936		897
<b>average (mid)</b>	<b>1.0156 (6)</b>				<b>1.151 (10)</b>			
HYD-87-03	1.0119 (8)	0.987		1233	1.123 (9)	0.988		1233
HYD-99-04	1.0135 (10)	0.964	15	1486	1.122 (12)	0.947		1486
<b>average (subtropics)</b>	<b>1.0127 (11)</b>				<b>1.122 (1)</b>			
<b>average (all latitudes)</b>	<b>1.0147 (2)</b>				<b>1.137 (14)</b>			

## The isotopic composition of methane in the stratosphere

T. Röckmann et al.

Title Page

Abstract

Introduction

Conclusions

References

Tables

Figures

◀

▶

◀

▶

Back

Close

Full Screen / Esc

Printer-friendly Version

Interactive Discussion

**Table 4.** Previously published mean KIE values.

Location		max. altitude	year-month	KIE <sup>13C</sup>	KIE <sup>D</sup>	Reference
Antarctica supply	Aircraft	12	1993-06	1.012		Brenninkmeijer et al. (1995)
Antarctica supply	Aircraft	12	1993-10	1.010		Brenninkmeijer et al. (1996)
Japan	Balloon	34.7	1994-08	1.0131 (6)		Sugawara et al. (1997)
STRAT, POLARIS, SOLVE	Aircraft	21	1996-09 to 2000-03	1.0154 (8)	1.153 (10)	Rice et al. (2003), overall average (2 $\sigma$ )

## The isotopic composition of methane in the stratosphere

T. Röckmann et al.

Title Page

Abstract

Introduction

Conclusions

References

Tables

Figures

⏪

⏩

◀

▶

Back

Close

Full Screen / Esc

Printer-friendly Version

Interactive Discussion



**Table 5.** Mean fractionation constants, corrected for tropospheric trends. The absolute differences in ‰ and the relative change in % to the uncorrected fractionation constants are stated in the right columns.

Set	$C_{\min}$ ppb	$\epsilon^{13C}$ ‰	$C_{\min}$ ppb	$\epsilon^D$ ‰	changes abs.		changes rel.	
					$\Delta$ [‰]	$\Delta$ [‰]	[%]	[%]
KIR-00-01	248	17.2	(248)*	(160)*	0.2		1.4	
KIR-92-01	265	16.6	335	151	0.5	9	2.8	6.1
KIR-92-02	272	16.1	272	135	0.4	6	2.7	4.9
KIR-92-03	397	14.9	397	135	0.5	7	3.2	5.7
KIR-03-03	271	17.2	271	137	0.4	3	2.4	2.6
KIR-03-06	652	17.0	652	152	0.2	6	1.4	4.1
ASA-93-09	831	16.2	613	163	0.9	4	5.9	2.2
KIR-95-03	835	15.7	835	161	0.8	16	5.6	10.7
GAP-99-06	631	17.0	631	162	0.4	9	2.6	5.9
ASA-01-10	957	15.8	(957)*	(159)*	0.5		3.3	
ASA-02-09	897	15.5	897	152	0.4	12	2.8	8.3
HYD-87-03	1233	13.6	1233	152	1.7	30	14.6	24.0
HYD-99-04	1486	14.5	1486	147	1.1	25	7.9	20.5

\* Using pseudo data, i.e. calculated  $\delta D$ -values according to the  $\delta D - \delta^{13C}$  correlation (1).

## The isotopic composition of methane in the stratosphere

T. Röckmann et al.

**Table 6.** Global mean dynamical factors  $f^{13\text{C}}$  and  $f^{\text{D}}$  (with errors) inferred from the modelled sink partitioning and the averaged mean fractionation factors.

average		$\epsilon^{13\text{C}}$		$\epsilon^{\text{D}}$		$f^{13\text{C}}$		$f^{\text{D}}$		$f_r$	
1	subtropics	14.0	0.7	150	4	0.553	0.026	0.456	0.011	0.82	0.04
2	mid-latitudes	16.1	0.6	159	5	0.635	0.025	0.484	0.016	0.76	0.04
3	non-vortex	16.3	0.9	157	6	0.643	0.037	0.478	0.019	0.74	0.05
4	vortex	16.2	1.0	144	10	0.639	0.038	0.437	0.031	0.68	0.06
5	polar <sup>1</sup> (3/4)	16.3	0.9	147	11	0.640	0.035	0.447	0.033	0.70	0.06
6	Global <sup>2</sup> (1/2/5)	15.5	1.2	152	6	0.610	0.049	0.462	0.019	0.76	0.07

<sup>1</sup> Polar: average of rows 3 and 4;

<sup>2</sup> Global: average of rows 1,2 and 5.

Title Page

Abstract

Introduction

Conclusions

References

Tables

Figures

⏪

⏩

◀

▶

Back

Close

Full Screen / Esc

Printer-friendly Version

Interactive Discussion

## The isotopic composition of methane in the stratosphere

T. Röckmann et al.

**Table 7.** Final fractionation for permuting three distinct Rayleigh-fractionation processes. The simulated  $\delta$ -values are different which shows that  $KIE_{\text{final}}$  is pathway dependent. Case 7 is a parallel removal by all three sink processes of equal strength, i.e.  $KIE_{\text{eff}}$  is constant along the fractionation pathway.

case	permutation	$\delta^{13}\text{C}$	$\delta\text{D}$	$KIE^{13}\text{C}$	$KIE^{\text{D}}$	$a_{\text{OH}}$	$a_{\text{O}^1\text{D}}$	$a_{\text{Cl}}$
1	OH-O( <sup>1</sup> D)-Cl	-24.3	93	1.035	1.327	0.18	0.44	0.39
2	O( <sup>1</sup> D)-Cl-OH	-28.9	95	1.028	1.330	0.35	0.35	0.30
3	Cl-OH-O( <sup>1</sup> D)	-30.7	65	1.026	1.264	0.24	0.52	0.24
4	Cl-O( <sup>1</sup> D)-OH	-31.2	80	1.025	1.297	0.35	0.41	0.24
5	OH-Cl-O( <sup>1</sup> D)	-28.0	70	1.030	1.275	0.17	0.53	0.29
6	O( <sup>1</sup> D)-OH-Cl	-24.6	103	1.035	1.349	0.25	0.36	0.39
7	3×1/3	-27.3	101	1.031	1.345	0.33	0.33	0.33

Title Page

Abstract

Introduction

Conclusions

References

Tables

Figures

⏪

⏩

◀

▶

Back

Close

Full Screen / Esc

Printer-friendly Version

Interactive Discussion

**Table 8.** results for  $f^{US}$  and  $x^{LS}$  assuming an additional OH sink in the lower stratosphere in case of  $a^{LS}(Cl) = 0$ . Results for KIR-00-01 and ASA-01-10 rely on pseudo- $\delta D$  profiles ((P), using Eq. 1) and ASA-02-09 has only a limited number of  $\delta D$  samples.

Flight	$x^{LS}$	$\epsilon_{\text{mean}}^{13C}$	$\epsilon_{\text{mean}}^D$	$a_{OH}$ (US)	$a_{O^1D}$ (US)	$a_{Cl}$ (US)	$x^{LS}$	$f^{US}$
HYD-87-03	0.13	13.6	152.4	0.32	0.38	0.30	0.13	0.472
HYD-99-04	0.22	14.5	147.1	0.25	0.42	0.33	0.22	0.463
ASA-93-09	0.22	16.2	163.1	0.24	0.42	0.33	0.22	0.514
GAP-99-06	0.26	17.0	162.2	0.20	0.45	0.35	0.26	0.515
ASA-01-10	0.22	15.8	159.1 (P)	0.24	0.42	0.33	0.22	0.501
ASA-02-09	0.25	15.5	151.6	0.22	0.44	0.34	0.25	0.479
KIR-95-03	0.20	15.7	161.4	0.26	0.41	0.33	0.20	0.506
KIR-03-06	0.30	17.0	152.4	0.15	0.47	0.37	0.30	0.489
KIR-92-01	0.30	16.6	151.0	0.16	0.47	0.37	0.30	0.483
KIR-92-02	0.35	16.1	134.9	0.10	0.51	0.40	0.35	0.438
KIR-92-03	0.30	14.9	135.2	0.16	0.47	0.37	0.30	0.433
KIR-00-01	0.28	17.2	160.3 (P)	0.18	0.46	0.36	0.28	0.511
KIR-03-03	0.38	17.2	136.6	0.05	0.53	0.42	0.38	0.448

## The isotopic composition of methane in the stratosphere

T. Röckmann et al.

Title Page

Abstract

Introduction

Conclusions

References

Tables

Figures

◀

▶

◀

▶

Back

Close

Full Screen / Esc

Printer-friendly Version

Interactive Discussion

## The isotopic composition of methane in the stratosphere

T. Röckmann et al.

Title Page

Abstract

Introduction

Conclusions

References

Tables

Figures

⏪

⏩

◀

▶

Back

Close

Full Screen / Esc

Printer-friendly Version

Interactive Discussion

**Table 9.** Coefficients of the piecewise polynomial approximation of methane loss rate estimation.

c-Interval [ppm]	polynomial factors				
	$A_4$	$A_3$	$A_2$	$A_1$	$A_0$
> 1.50	65.08	-399.36	916.01	-930.59	353.13
1.50–1.06	0	-0.87	3.95	-5.45	2.12
< 1.06	-5.26	14.23	-12.77	7.07	-3.71

## The isotopic composition of methane in the stratosphere

T. Röckmann et al.

**Table 10.** Comparison of two samples at the upper stratospheric border. KIR-03-03/6 is found on the vortex branch of the isotope:isotope relation. It is evident that KIR-03-03/12 must have experienced a different fractionation/mixing history. Although its methane mixing ratio is higher than that of KIR-03-03/6, it is much more enriched. Interpreting KIR-03-03/12 as a result of an end-member mixing process between mesospheric influenced vortex air and upper stratospheric mid-latitude air, an appropriate upper stratospheric end-member is reconstructed (KIR-03-03/US).

KIR-03-03 #	altitude km	c ppb		$\delta^{13}\text{C}$ ‰		$\delta\text{D}$ ‰		
6	23.9	271	1.8	-17.91	0.14	143.1	11	vortex sample, mesospheric influence mix
12	22.5	291	0.4	-13.70	0.67	191.3	2.4	
US	~40 <sup>1</sup>	314		-9.35		241.1		hypothetical mid-latitude upper stratosphere

\* Estimated from typical mid-latitude profile.

[Title Page](#)
[Abstract](#)
[Introduction](#)
[Conclusions](#)
[References](#)
[Tables](#)
[Figures](#)
[Back](#)
[Close](#)
[Full Screen / Esc](#)
[Printer-friendly Version](#)
[Interactive Discussion](#)


## The isotopic composition of methane in the stratosphere

T. Röckmann et al.

Title Page

Abstract

Introduction

Conclusions

References

Tables

Figures

◀

▶

◀

▶

Back

Close

Full Screen / Esc

Printer-friendly Version

Interactive Discussion

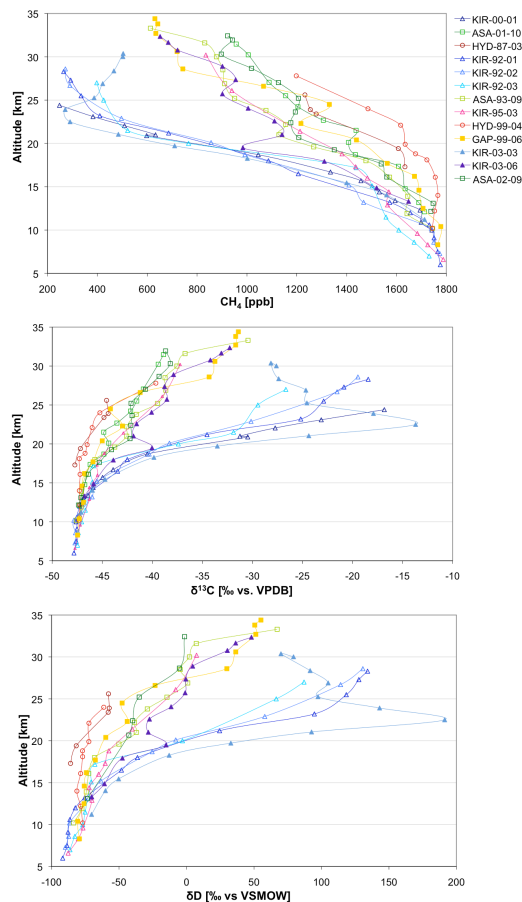


**Fig. 1.** Methane mixing ratio (a),  $\delta^{13}\text{C}$  (b) and  $\delta\text{D}$  (c) for all analysed balloon samples.  $\Delta$ : Arctic samples (blue: vortex, purple: non-vortex, solid symbols: flight with mesospheric influence),  $\square$ : mid-latitudes (green, yellow),  $\circ$ : tropics (red), solid symbols: sampled in summer.

## The isotopic composition of methane in the stratosphere

T. Röckmann et al.

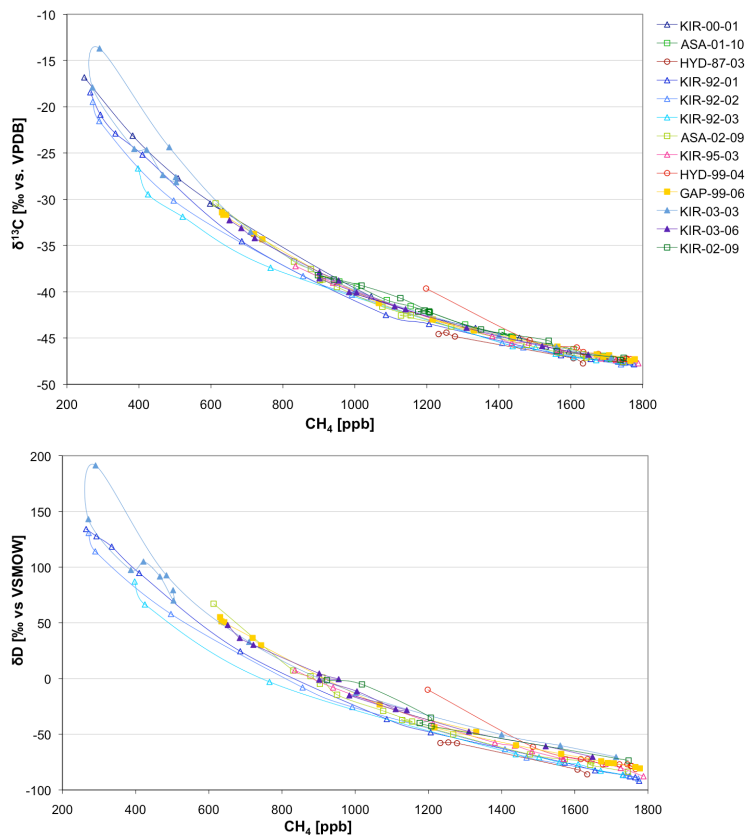


**Fig. 2.** Isotope:tracer relations  $\delta(c)$  for the balloon data shown in Fig. 1.

[Title Page](#)[Abstract](#)[Introduction](#)[Conclusions](#)[References](#)[Tables](#)[Figures](#)[◀](#)[▶](#)[◀](#)[▶](#)[Back](#)[Close](#)[Full Screen / Esc](#)[Printer-friendly Version](#)[Interactive Discussion](#)

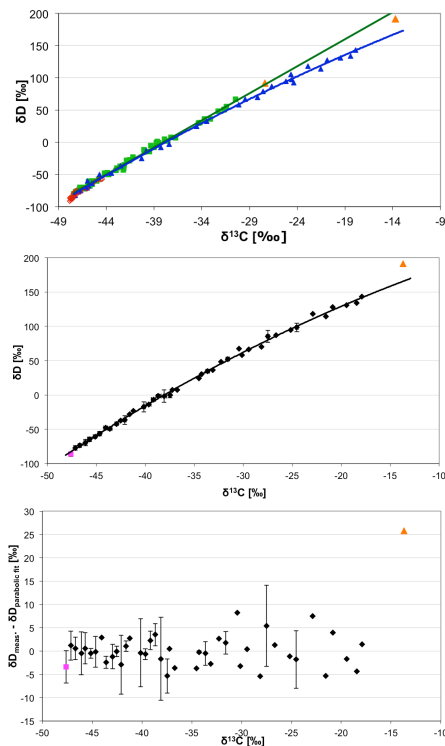


**Fig. 3.** Isotope-isotope correlation **(a)** for tropical (red) mid-latitude (green) and polar (blue) samples, exceptional samples from KIR-03-03 ( $\Delta$ ) in orange. Mid-latitude samples follow a linear fit, whereas polar samples follow a parabolic fit. The parabolic shape dominates in the fit to all data **(b)**. Here, the data was binned in 0.5‰  $\delta^{13}\text{C}$  intervals to reduce the statistical weight of the more abundant higher mixing ratio (lower  $\delta$ -values) samples. The residuals between parabolic fit and data **(c)**, excluding the highest enrichment point, show no systematic structure. The error bars represent typical variations in a 0.5‰  $\delta^{13}\text{C}$  bin.

**The isotopic composition of methane in the stratosphere**

T. Röckmann et al.

Title Page

Abstract Introduction

Conclusions References

Tables Figures

◀ ▶

◀ ▶

Back Close

Full Screen / Esc

Printer-friendly Version

Interactive Discussion



## The isotopic composition of methane in the stratosphere

T. Röckmann et al.

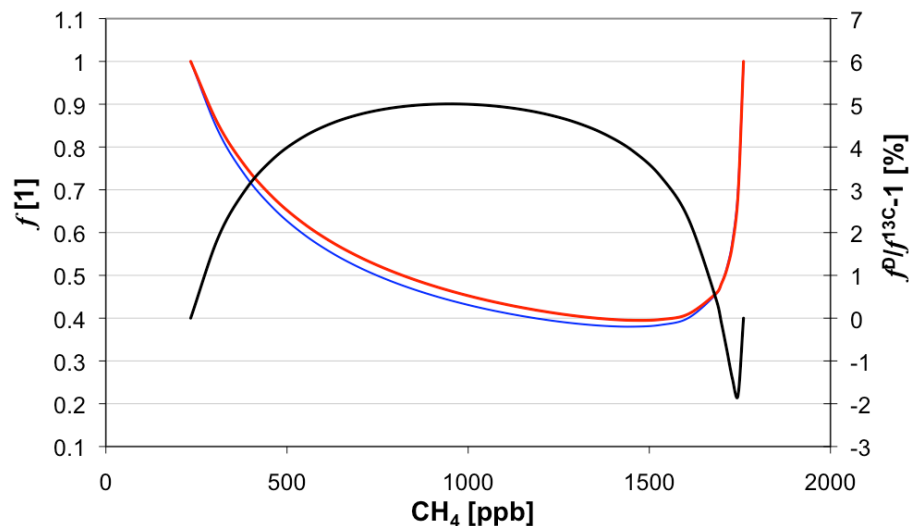


**Fig. 4.** Attenuation effect of end-member mixing on two representative Rayleigh fractionation lines (carbon  $\epsilon^{13\text{C}} = 29\text{‰}$  and hydrogen  $\epsilon^{\text{D}} = 250\text{‰}$ ), expressed by  $f$ -values ( $f^{13\text{C}}$  (blue) and  $f^{\text{D}}$  (red), left scale). The two end members ( $c_1 = 1760$  ppb,  $c_2 = 234$  ppb) for mixing were derived from an initial mixing ratio  $c_0 = 1780$  ppb. The black line shows the relative difference of the effect on hydrogen to carbon (right scale).

[Title Page](#)
[Abstract](#)
[Introduction](#)
[Conclusions](#)
[References](#)
[Tables](#)
[Figures](#)
[◀](#)
[▶](#)
[◀](#)
[▶](#)
[Back](#)
[Close](#)
[Full Screen / Esc](#)
[Printer-friendly Version](#)
[Interactive Discussion](#)

## The isotopic composition of methane in the stratosphere

T. Röckmann et al.

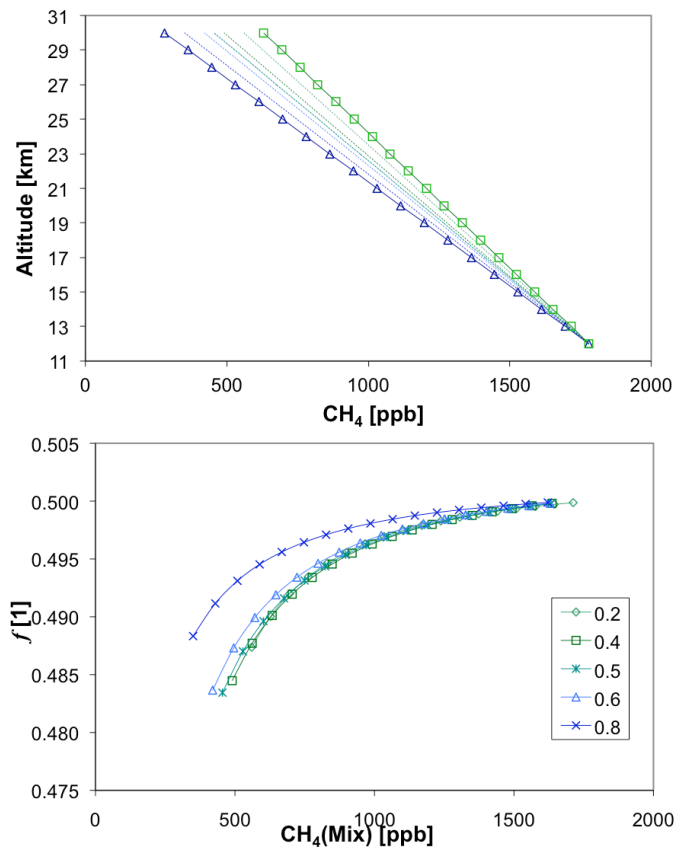


**Fig. 5.** (a) Idealized CH<sub>4</sub> vertical profiles for idealized vortex (Δ, blue) and mid-latitude (□, green) air and mixing of the two end members (fraction of vortex air, see legend in (b)). (b) resulting *f*-values derived from the mean KIE up to the altitude where the symbol is drawn, i.e. from one point to the next, air from the next altitude is included in the calculation of the mean KIE.

## The isotopic composition of methane in the stratosphere

T. Röckmann et al.

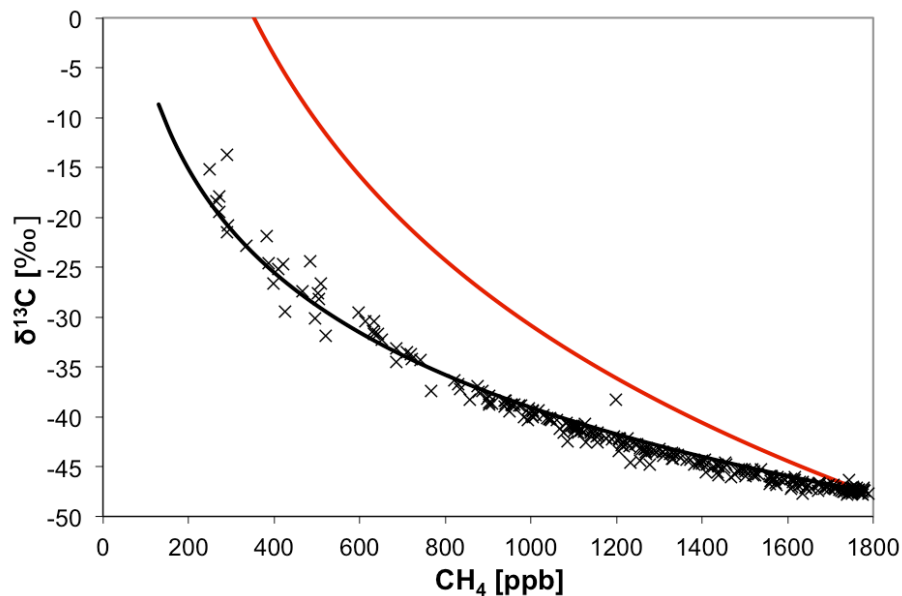


**Fig. 6.** Comparison of theoretical Rayleigh fractionation (red,  $\varepsilon = 31\text{‰}$ ) and the prediction of the 1-D-diffusive model (black,  $f = 0.5$ ,  $\varepsilon = 15.5\text{‰}$ ) to the observed  $\delta^{13}\text{C}$ -values.

[Title Page](#)[Abstract](#)[Introduction](#)[Conclusions](#)[References](#)[Tables](#)[Figures](#)[⏪](#)[⏩](#)[◀](#)[▶](#)[Back](#)[Close](#)[Full Screen / Esc](#)[Printer-friendly Version](#)[Interactive Discussion](#)

## The isotopic composition of methane in the stratosphere

T. Röckmann et al.

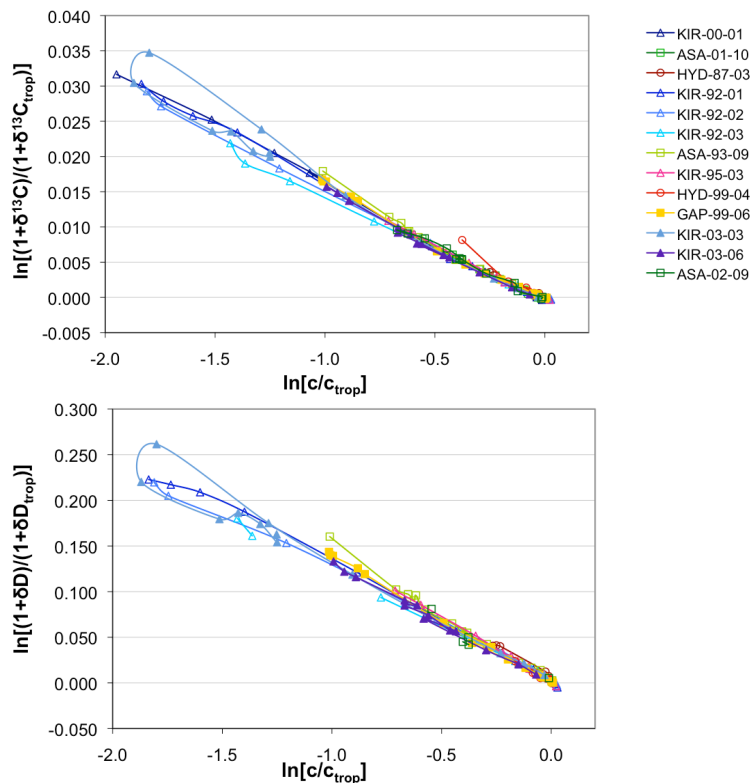


**Fig. 7.** Rayleigh plots used for deriving the mean fractionation factors for  $\delta^{13}\text{C}$  and  $\delta\text{D}$ . Some exceptional points have been neglected for the fitting procedure. The lines in the graphs connect the points of each flight according to the sampling altitude. Regression lines are left out, since the principal linear dependence is obvious.

[Title Page](#)
[Abstract](#)
[Introduction](#)
[Conclusions](#)
[References](#)
[Tables](#)
[Figures](#)
[Back](#)
[Close](#)
[Full Screen / Esc](#)
[Printer-friendly Version](#)
[Interactive Discussion](#)

## The isotopic composition of methane in the stratosphere

T. Röckmann et al.

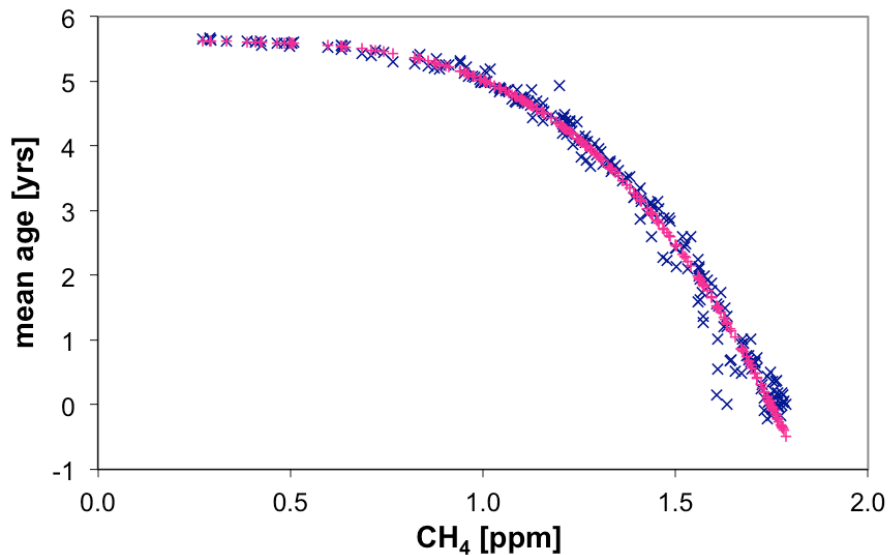


**Fig. 8.** Stratospheric mean age plotted versus CH<sub>4</sub> mixing ratio (red, “+”). The original age inferred from the N<sub>2</sub>O mixing ratio is shown in blue (“-”).

[Title Page](#)[Abstract](#)[Introduction](#)[Conclusions](#)[References](#)[Tables](#)[Figures](#)[⏪](#)[⏩](#)[◀](#)[▶](#)[Back](#)[Close](#)[Full Screen / Esc](#)[Printer-friendly Version](#)[Interactive Discussion](#)

## The isotopic composition of methane in the stratosphere

T. Röckmann et al.

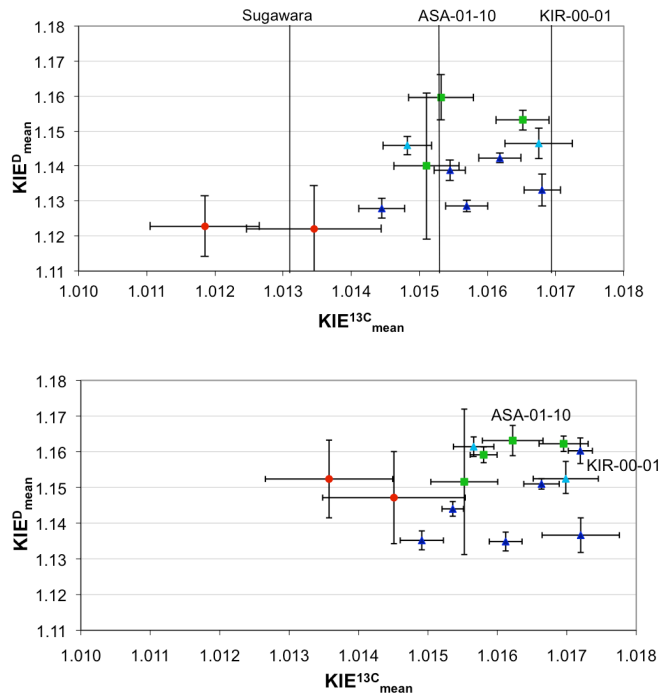


**Fig. 9.** Mean KIE determined before (upper panel) and after (lower panel) applying the correction for tropospheric trends. Errors result from fit uncertainty. Flights are grouped and colour-coded according to their cut-off bias (subtropical: red ●; mid-latitudes: green ■; Arctic vortex: dark blue ▲ and Arctic non-vortex: light blue ▲). KIR-00-01 and ASA-01-10 in the bottom figure are based on pseudo- $\delta D$  values calculated from the isotope:isotope correlation. In the top figure only the real KIE<sup>13C</sup> values are shown for those flights, indicated by vertical lines. Additionally, the only previous published balloon profile (<sup>13C</sup> only) from Sugawara et al. (1997) is included for direct comparison to the other flights.

Title Page

Abstract

Introduction

Conclusions

References

Tables

Figures

◀

▶

◀

▶

Back

Close

Full Screen / Esc

Printer-friendly Version

Interactive Discussion

## The isotopic composition of methane in the stratosphere

T. Röckmann et al.

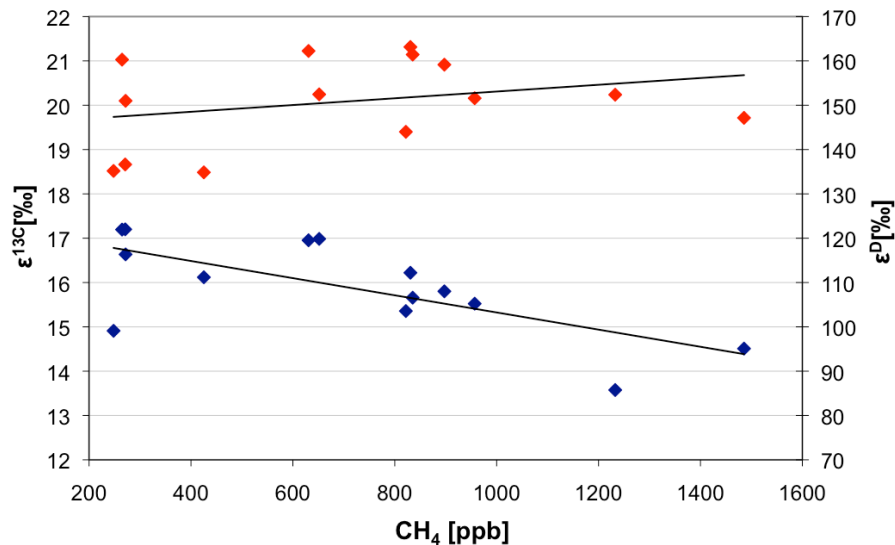


**Fig. 10.** Dependence of mean fractionation factors of each flight ( $\epsilon^{13}\text{C}$  in blue,  $\epsilon^{\text{D}}$  in red) on the corresponding lowest mixing ratio  $c_{\text{min}}$  observed. Fractionation factors are taken from Table 5 and include the correction for the tropospheric temporal trends.

[Title Page](#)
[Abstract](#)
[Introduction](#)
[Conclusions](#)
[References](#)
[Tables](#)
[Figures](#)
[⏪](#)
[⏩](#)
[◀](#)
[▶](#)
[Back](#)
[Close](#)
[Full Screen / Esc](#)
[Printer-friendly Version](#)
[Interactive Discussion](#)


**The isotopic composition of methane in the stratosphere**

T. Röckmann et al.

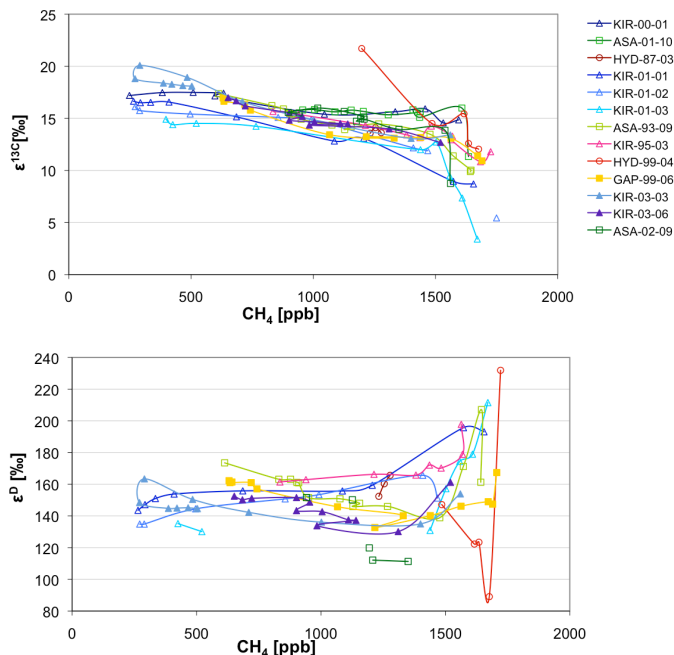


**Fig. 11.** The bottom-up profiles show the increase in  $\epsilon^{13}\text{C}$  with decreasing  $c_{\text{min}}$ , which illustrates the decreasing importance of OH with increasing altitude (decreasing mixing ratio) and reduction of  $\delta\text{D}$  relative to  $\delta^{13}\text{C}$  in the vortex. Some data points that include only lower stratospheric samples have been left out in the graphs, since they reflect tropospheric variations. The last data point (on the left side) of each line corresponds to the  $\text{KIE}_{\text{mean}}$  results of Table 5, but as exceptional samples have not been excluded here, they can slightly differ from the values given there. Typically the topmost sample has the lowest methane mixing ratio in a profile and therefore defines  $c_{\text{min}}$ . The major exception is KIR-03-03 (light blue), which has a minimum in the vertical mixing ratio profile, so that instead of  $c_{\text{min}}$  the mixing ratio of the topmost sample characterises the related mean fractionation factor.

Title Page

Abstract	Introduction
Conclusions	References
Tables	Figures

⏪      ⏩  
◀      ▶

Back	Close
------	-------

Full Screen / Esc

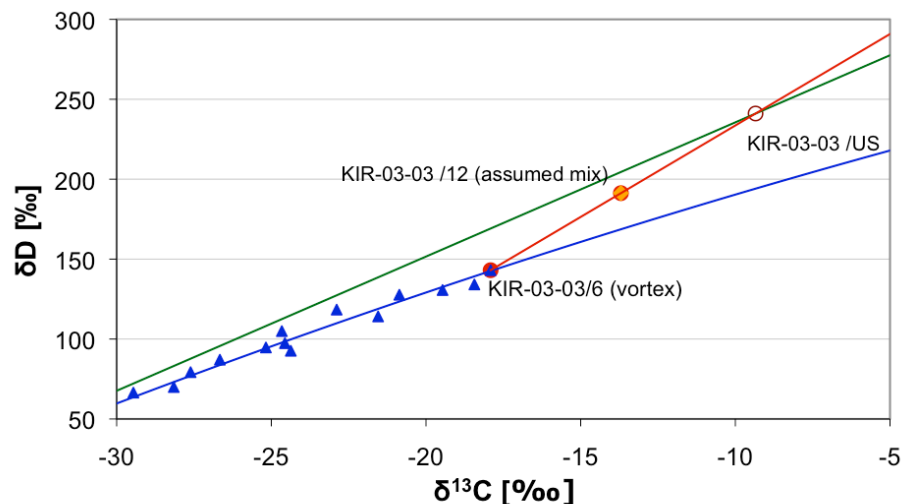
Printer-friendly Version

Interactive Discussion



## The isotopic composition of methane in the stratosphere

T. Röckmann et al.

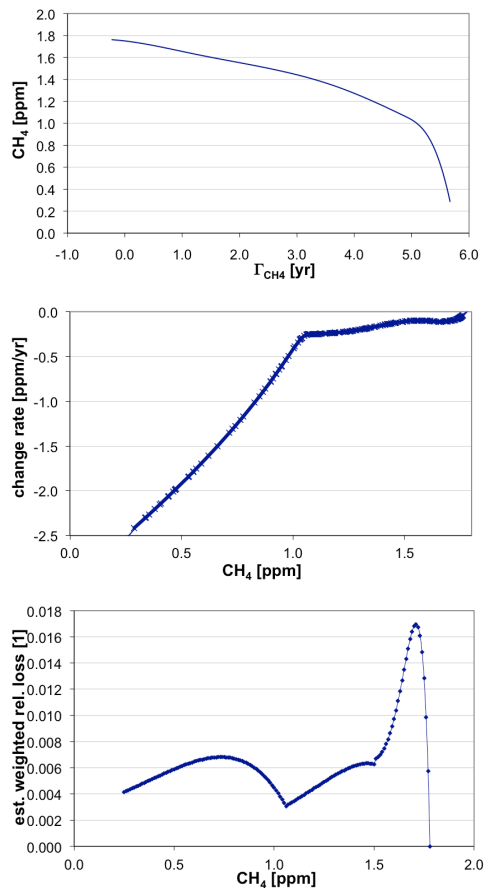


**Fig. 12.** Assuming that KIR-03-03/12 is the result of an end-member mixing process between vortex air (blue) and upper stratospheric air outside the vortex (green), an appropriate upper stratospheric member KIR-03-03/US can be constructed.

[Title Page](#)[Abstract](#)[Introduction](#)[Conclusions](#)[References](#)[Tables](#)[Figures](#)[◀](#)[▶](#)[◀](#)[▶](#)[Back](#)[Close](#)[Full Screen / Esc](#)[Printer-friendly Version](#)[Interactive Discussion](#)

## The isotopic composition of methane in the stratosphere

T. Röckmann et al.

[Title Page](#)[Abstract](#)[Introduction](#)[Conclusions](#)[References](#)[Tables](#)[Figures](#)[◀](#)[▶](#)[◀](#)[▶](#)[Back](#)[Close](#)[Full Screen / Esc](#)[Printer-friendly Version](#)[Interactive Discussion](#)

**Fig. 13.** (a) CH<sub>4</sub> mixing ratio as a function of the mean age  $\Gamma$ ; (b) first derivative, used as independent estimate for the loss rate; (c) relative (normalized) part of the estimated loss as a function of mixing ratio.